Translational Oncology

www.transonc.com

Volume 4 Number 3 June 2011 pp. 157–172 157

Molecular Validation of PACE4 as a Target in Prostate Cancer[1,2]

François D'Anjou*, Sophie Routhier*, Jean-Pierre Perreault†, Alain Latil‡,3, David Bonnel*,§, Isabelle Fournier§, Michel Salzet§ and Robert Day*

*Institut de Pharmacologie de Sherbrooke, Université de Sherbrooke, Sherbrooke, Québec, Canada; †Département de Biochimie, Université de Sherbrooke, Sherbrooke, Québec, Canada; ‡Urogene, Génopole, Evry Cedex, France; §Université Nord de France, Centre National de la Recherche Scientifique, MALDI Imaging team, Laboratoire de spectrométrie de masse biologique fondamentale et appliquée, Villeneuve d'Ascq, France

Abstract

Prostate cancer remains the single most prevalent cancer in men. Standard therapies are still limited and include androgen ablation that initially causes tumor regression. However, tumor cells eventually relapse and develop into a hormone-refractory prostate cancer. One of the current challenges in this disease is to define new therapeutic targets, which have been virtually unchanged in the past 30 years. Recent studies have suggested that the family of enzymes known as the proprotein convertases (PCs) is involved in various types of cancers and their progression. The present study examined PC expression in prostate cancer and validates one PC, namely PACE4, as a target. The evidence includes the observed high expression of PACE4 in all different clinical stages of human prostate tumor tissues. Gene silencing studies targeting PACE4 in the DU145 prostate cancer cell line produced cells (cell line 4-2) with slower proliferation rates, reduced clonogenic activity, and inability to grow as xenografts in nude mice. Gene expression and proteomic profiling of the 4-2 cell line reveals an increased expression of known cancer-related genes (e.g., *GJA1*, *CD44*, *IGFBP6*) that are downregulated in prostate cancer. Similarly, cancer genes whose expression is decreased in the 4-2 cell line were upregulated in prostate cancer (e.g., *MUC1*, *IL6*). The direct role of PACE4 in prostate cancer is most likely through the upregulated processing of growth factors or through the aberrant processing of growth factors leading to sustained cancer progression, suggesting that PACE4 holds a central role in prostate cancer.

Translational Oncology (2011) 4, 157–172

Address all correspondence to: Dr. Robert Day, Institut de Pharmacologie de Sherbrooke, Faculté de Médecine et des Sciences de la Santé, Université de Sherbrooke, 3001 12e Ave. Nord, Sherbrooke, Québec, Canada J1H 5N4. E-mail: robert.day@usherbrooke.ca

[1]This work was funded by grants from the Canadian Institutes of Health Research, the Ministère du Développement Économique de l'Innovation et de l'Exportation (to R.D.), the Centre National de la Recherche Scientifique (to M.S. and I.F.), and the Agence Nationale de la Recherche (to I.F.) and scholarships from Natural Sciences and Engineering Research Council of Canada (to F.D. and S.R.) and from Fonds de la Recherche en Santé du Québec (to F.D.). R.D. is a member of the Centre de Recherche Clinique Etienne-Le Bel (Sherbrooke, Québec, Canada).

[2]This article refers to supplementary materials, which are designated by Tables W1 and W2 and are available online at www.transonc.com.

[3]Present address: Laboratoire de Microbiologie, Institut de Recherche Pierre Fabre, Toulouse, France.

Received 17 December 2010; Revised 2 February 2011; Accepted 14 February 2011

 1944-7124/11

DOI 10.1593/tlo.10295

Introduction

Cancer cells are characterized by multiple genetic alterations that confer physiological changes, leading to uncontrolled division and ability to invade other tissues [1]. These acquired capabilities, namely cell proliferation, tissue invasion, and adhesion, are essential for malignant growth and progression. Numerous studies have associated the family of enzymes known as the proprotein convertases (PCs) to cancer [2–8]. PCs are serine proteases that cleave substrates at R-X-K/R-R↓ motif [9,10]. These processing events, resulting in the activation of protein precursors, occur at multiple levels of cell secretory pathways, and even at the cell surface. In mammalian cells, seven basic amino acid cleaving members of this family have been identified: furin, PACE4, PC1/3, PC2, PC4, PC5/6, and PC7. PCs show differential expression levels within tissues, ranging from ubiquitous (e.g., furin) to an endocrine-restricted expression (e.g., PC1/3 and PC2).

The first association of PCs with cancer was done by comparative studies of normal and cancerous cells showing higher expression of PCs in small cell lung cancer [11], non–small cell lung carcinoma [12], breast [13], colon [14], and head and neck [15] tumor cells or lower expression in ovarian cancer [16]. A correlation between expression of some PCs, namely furin and PACE4, and tumor cells' aggressiveness has been established for different cell types [8,15,17–20]. Thus, it is hypothesized that through processing events, cancer cells have a higher capacity (i) to remodel the extracellular matrix (e.g., MT1-MMP and MT2-MMP; [17,21,22]), (ii) to interact with their host microenvironment to favor adhesion (e.g., IL-1α, TNF-α, and E-selectin [7]); and (iii) to modulate their proliferation and differentiation (e.g., IGF-1 receptor [7], VEGF-C, -D [23,24], PDGF-A, -B [24,25], TGF-β [26]). One possible mechanism whereby PCs are critical in cancer progression could be on the basis of differential precursors processing by overexpressed PCs. Alternatively, PCs overexpression is required to sustain pathophysiological functions to maintain cancer cells immortality, for example to sustain the processing of required growth factors or proangiogenic factors. Together, these studies suggest that PCs processing events are directly linked to tumor development by allowing cancer cells to maintain some of their acquired capabilities.

Because the PC family of enzymes is very large and often responsible for redundant processing functions, more precise studies are required if we are to understand their specific roles in different cancer types. Thus, there is a need for potent, specific, and cell-effective inhibitors, either pharmacologic or molecular, for each member of this enzyme family. Pharmacological tools are limited as many lack the required specificity for single PCs [9,27–30]. For example, a study by Uchida et al. [31] showed that treatment of prostate cancer cell lines with the general PC inhibitor decanoyl-Arg-Val-Lys-Arg-chloromethylketone (dec-RVKR-CMK) inhibited prostate-derived factor processing and resulted in the loss of luminal cell phenotype and induction of basal cell phenotype as demonstrated by alternations in the expression of cytokeratins 8, 14, 18, and 19, markers of prostate epithelial cell differentiation. Because dec-RVKR-CMK inhibits all PCs, the study could not distinguish which PCs expressed in the prostate cancer cell lines were more important. To ask the question as to which PCs are the most important for cancer progression, molecular approaches targeting specific PC messenger RNA (mRNA) are closer to achieving this goal. There are various sequence-specific approaches taking advantage of either endogenous ribonucleases (e.g., small interfering RNA [siRNA] and phosphorothioate antisense oligonucleotide) or their intrinsic catalytic activity (e.g., deoxyribozyme and ribozyme) to drive the degradation of the targeted RNA [32].

In the present study we chose to examine the role of PCs in prostate cancer. In men, prostate cancer accounts for the highest incident cases and the second most deadliest cancer type [33]. Because disease diagnosis and treatment have been little changed in the past 30 years, it is possible that a better understanding of the molecular events leading to advanced prostate cancer states could lead to the development of new, efficient, and targeted therapies [34]. We first evaluated the implication of each PC on different types of prostate cancer biopsies and detected the unique PACE4 mRNA overexpression. Based on these findings, we created a DU145 cell line model, using the switch on/off adapter-hepatitis delta virus ribozyme (SOFA-HDVRz) as a RNA silencing tool, to investigate PACE4's contribution in androgen-independent prostate cancer cells. The results of this study, based on *in vitro* assays, gene expression, and proteomic profiling, as well as animal studies, led us to the conclusion that PACE4 plays a critical role in the progression of prostate cancer and therefore could be a novel therapeutic target for its treatment.

Materials and Methods

Patients and Samples

Prostate tumor samples were obtained from either St Louis and Bichat Hospital (Paris, France) or Tournan's clinic (Tournan en Brie, France), as previously described [35]. Each patient included has signed the sample informed consent form. Sample tissues from the 34 patients with clinically localized prostate tumors were obtained by removing clinically localized tumors by radical prostatectomy and classified according to their clinical stage using the TNM system [36,37]. After pathological examination, 18 samples were at stage pT2, whereas 16 samples were at stage pT3. The sample tissues from hormone-refractory recurrent prostate carcinoma were obtained from patients with metastatic disease at diagnosis. Because these patients were not amenable to radical surgery, they received endocrine therapy, either by classic androgen deprivation (orchidectomy or luteinizing hormone–releasing hormone agonist administration) or by maximal androgen blockade (castration combined with antiandrogen therapy). These patients relapsed, and their tumors became clinically androgen-independent. The 13 samples of these hormone-refractory recurrent prostate carcinomas were obtained during transurethral resection. Suspect areas were examined histopathologically in the surgery suite, and thick shave sections were taken for research purposes. These preselected tumor specimen sections were then sliced on each side in the laboratory and again subjected to pathological examination. Confirmed areas were carefully microdissected using a scalpel and the assistance of an experienced pathologist. Well-characterized matched normal prostate specimens (nine samples) from the 34 patients with clinically localized prostate tumors who underwent radical prostatectomy were used to assess basal target gene mRNA expression. Normal-looking areas of each surgical specimens were examined histologically for the absence of cancer cells and selected on their microscopic pathological criteria to avoid the inclusion of areas with benign hyperplasia. Normal specimens were then proceeded as previously described for tumor tissues.

Real-time Polymerase Chain Reaction on Tissues

The RNA was extracted from dissected tissues with an acid-phenol guanidium method, reverse-transcribed, and submitted to quantitative

polymerase chain reaction (PCR) as previously described [35]. A genomic DNA and nontemplate control were included in each experiment. Samples and controls were tested in duplicate. The threshold cycle (C_t) numbers obtained from PCR amplifications were expressed as fold change in target gene expression (PACE4) relative to an endogenous control gene (*PPIA*; peptidyl prolyl isomerase A gene encoding cyclophilin A). The primer sequences for endogenous control gene *PPIA* (the peptidyl prolyl isomerase A gene encoding cyclophilin A) were described earlier [35]. The primer sequences were as follows: PACE4 sense, 5′-CAAGAGACCCAGGAGCATCCC-3′; PACE4 antisense, 5′-ACCCGCTGGTCCGAGTGCT-3′; furin sense, 5′-CCAGGATGAATCCCAGGTGCTC-3′; furin antisense, 5′-GGAGGGTGAAGAGTGCCGACC-3′; PC7 sense, 5′-CATCCAGGACATTGCACCCAAC-3′; and PC7 antisense, 5′-GGTTGCCATTCTCCACATCCG-3′.

In Situ *Hydridization*

The *in situ* hydridization protocol using digoxigenin-labeled complementary RNA probes have been described in details previously [38].

SOFA-HDVRz Design, Cloning, and In Vitro *Cleavage Assays*

Bioinformatic analysis. Human PACE4 complementary DNA (cDNA) sequence (M80482) was used for the determination of the optimal SOFA-HDVRz targeting site. The selection criteria were (i) the first nucleotide (nt) should be a G to form the required wobble bp within the P1 stem; (ii) after the 6 subsequent nt of the P1 stem, a 5 nt spacer was added; and (iii) a 12-nt biosensor stem was used to complete the design. Thus, the targeted site on cDNA was 5′ $(GN_6)_{P1}$-$(N_5)_{Spacer}$-$(N_{12})_{Biosensor}$-3′ (Figure 2*A*). We focused our search for optimal cleavage site within the first 1200 nt of the PACE4 cDNA and tested several potential targeting sites with the Ribosubstrates online software (http://www.riboclub.org/ribosubstrates) [39]. This integrated software searches in selected cDNA databases all potential substrates for a given SOFA-HDVRz. These potential substrates include mRNA with perfect matches with the catalytic RNA tested, but also the wobble bp and mismatches. Only SOFA-HDVRz with a human PACE4-specific biosensor and harboring a minimum of wobble bp were considered.

Plasmid DNA constructs. As previously detailed [40], we used the expression vector ptRNA^{Val}/hygromycin containing the RNA polymerase III promoter tRNA^{Val} promoter for cellular applications. A PCR strategy was used to create a DNA template containing a 5′-*Kpn*I restriction site and a 3′-blunt end. The sequences of the two complementary and overlapping DNA oligodeoxynucleotides used were as follows: sense, 5′-ATCCATCGGGTACCGGGCCAGCTAGTTT $(GGCCTCTGCTAC)_{BS}(CAAC)_{BL}$CAGGGTCCACC-3′ and, antisense, 5′-CCAGCTAGAAAGGGTCCCTTAGCCATCCGCGAACGGATGCCCA$(ATCAAC)_{P1}$ACCGCGAGGAGGTGGACCCTG $(GTTG)_{BL}$-3′. The underlined nt correspond to the *Kpn*I restriction site, and those in parenthesis to the PACE4 specific biosensor (BS), blocker (BL) and P1 stem (P1) of the PACE4-SOFA-HDVRz. The purified and *Kpn*I-digested PCR product was cloned in the expression vector previously digested with *Kpn*I and *Eco*RV restriction enzymes. The vector used to restore PACE4 mRNA expression level contained the full-length PACE4 cDNA and a neomycin resistance gene (kindly provided by Dr J.W. Creemers [41]).

RNA synthesis. As previously described, radiolabeled PACE4 RNA was obtained from transcription of an *Xho*I-digested pcDNA3 vector containing a chimeric cDNA composed of the PC5/6A signal peptide linked to proPACE4 coding sequence [41] using T7 RNA polymerase with 50 μCi of [α-^{32}P]GTP [40]. The catalytic RNA were synthesized using a PCR-based strategy with the expression vectors to generate DNA templates containing a 5′-T7 RNA polymerase promoter using either the following sense primer 5′-TTAATACGACTCACTATAGGGACCGTTGGTTTCCGTAG-3′ or 5′-TTAATACGACTCACTATAGGGCCAGCTAGTTT-3′, complementary to the tRNA^{Val} promoter or the PACE4-SOFA-HDVRz, respectively (the underlined nucleotides correspond to the T7 RNA polymerase promoter sequence). The antisense oligodeoxynucleotide sequence used for both PCR was 5′-CCAGCTAGAAAGGGTCCCTTA-3′. After PCR, the purified products were used as templates for T7 RNA polymerase transcription of tRNA^{Val}-PACE4-SOFA-HDVRz or PACE4-SOFA-HDVRz, as described previously [40]. All products were purified on denaturing 5% (PACE4 transcript) or 7.5% (for PACE4-SOFA-HDVRz transcripts) PAGE.

Cleavage assay. The SOFA-HDVRz cleavage assays under single turnover conditions ([SOFA-HDVRz] > [PACE4 RNA]) were done at 37°C for 3 hours in a 10-μl reaction containing trace amount of radiolabeled PACE4 RNA and 1 μM of SOFA-HDVRz in reaction buffer containing 50 mM Tris-HCl, pH 7.5, and 10 mM $MgCl_2$. The reactions were stopped by the addition of loading buffer (97% formamide, 1 mM EDTA [pH 8.0], 0.025% xylene cyanol and 0.025% bromophenol blue), electrophoresed on denaturing 5% PAGE gel, and analyzed with a PhosphorImager (Amersham Biosciences, Sunnyvale, CA).

Cell Culture and DNA Transfection

Human cancer prostate cell lines DU145 were obtained from ATCC (Manassas, VA). Cells were maintained in Roswell Park Memorial Institute medium (RPMI 1640) supplemented with 5% fetal bovine serum (Wisent Bioproducts, St-Jean-Baptiste, Quebec, Canada). Cells were grown at 37°C in a water-saturated atmosphere in air/CO_2 (5%). Cells were transfected using Lipofectamine 2000 (Invitrogen, Burlington, Ontario, Canada) as per manufacturer's instruction and were selected for resistance to hygromycin B (Invitrogen) at 125 μg/ml, with 200 μg/ml of neomycin for double-transfected cells. The stable cell line transfected with the SOFA-HDVRz expression vector was named 4-2, whereas the 4-2 cell line stably transfected with the PACE4 expression vector was named 4-2 + PACE4.

Northern Blot Hybridizations

RNA extractions and Northern blots were performed as previously described [40]. The 1066-bp cDNA for human furin probe was obtained by digestion of the full-length clone with *Xho*I enzyme [42]. A 456-bp cDNA fragment of PACE4 was cloned in pGEM-T easy vector system (Promega, Madison, WI) by reverse transcription–PCR on DU145 total RNA with specific primers [13]. This vector was subsequently used for probe transcription. For the PC7 probe, we used a 285-bp rat cDNA [43], and for bovine 18S ribosomal RNA probe, a 600-bp cDNA [44] was used. The ImageJ software 1.37v (http://rsb.info.nih.gov/ij/) was used for all densitometric analyses.

Microarray Analysis

Sample preparation. RNA from DU145 or 4-2 cell pellets (in duplicate) was extracted using TRIzol reagent (Invitrogen) according to the manufacturer's instructions and purified using RNeasy mini kit (Qiagen, Mississauga, Ontario, Canada). The quality of the RNA was assessed using a 2100 Bioanalyzer with the RNA 6000 Nano LabChip kit (Agilent Technologies, Mississauga, Ontario, Canada).

Data processing. The microarray hybridization and the data collection were performed on the Functional Genomics Platform of the McGill University and Genome Québec Innovation Centre (Montréal, Quebec, Canada) using Illumina whole genome Human WG-6 v3.0 bead chip (38,275 genes). The processing of data was done with the software FlexArray v1.2 (http://genomequebec.mcgill.ca/FlexArray/). Briefly, the raw data were preprocessed and normalized for each array using the "lumi" algorithm. Then, the mean fold changes of normalized data were calculated for DU145 *versus* 4-2. Statistical analysis was performed using the Significance Analysis of Microarrays method, which uses a modified *t* test statistic and sample-label permutations to evaluate statistical significance [45].

Real-time PCR validation. The real-time PCR assays were carried out on the Mx3000P quantitative PCR system using the Brilliant II SYBR Green kits (Stratagene, Cedar Creek, TX). Briefly, the RNA was DNase I–treated (Invitrogen), reverse-transcribed using Superscript II reverse transcriptase (Invitrogen), and RNaseH-treated (Ambion, Austin, TX) before quantitative PCR. The reaction mixtures combined 1 μg of cDNA with 12.5 μl of 2× master mix containing primers at a 300-nM final concentration. The PCR profile was one cycle for 10 minutes at 95°C, 40 cycles of 30 seconds at 95°C, 1 minute at 60°C, and 30 seconds at 72°C. Primers were designed using Beacon Designer software (http://www.premierbiosoft.com). The sequences of primers used were as follows: SERPINE2 (NM_006216), sense 5′-CCCACTTCAATCCTCTGTCTCTC-3′ and antisense 5′-CCCAGGACCGACGCAATC-3′; CDK6 (NM_001259), sense 5′-GCCGCCCAGCCAGAACAC-3′ and antisense 5′-CTCCAGATAGCAATCCTCCACAGC-3′; IGFBP6 (NM_002178), sense 5′-GCGTGGAGGAGGAGGATGG-3′ and antisense 5′-CTTGGGCGGATGGCACTG-3′; TGFBI (NM_000358), sense 5′-GTGCGGCTGCTGGCTCTC-3′ and antisense 5′-GCTGGTAGGGCGACTTGGC-3′; CCNA1 (NM_003914), sense 5′-YGAAGAAGCAGCCAGACATC-3′ and antisense 5′-AAGTTGACAGCCAGATACAGG-3′; IGFBP3 (NM_001013398), sense 5′-TTCTGCTGGTGTGTGGATAAG-3′ and antisense 5′-GGCGTCTACTTGCTCTGC-3′; THBS1 (NM_003246), sense 5′-GGACTCGCTGTAGGTTATGATG-3′ and antisense 5′-CGGCTGCTGGACTGGTAG-3′; MUC1 (NM_002456), sense 5′-CTGGTGCTGGTCTGTGTTC-3′ and antisense 5′-GCTGCCCGTAGTTCTTTCG-3′; and ACTB (NM_007393), sense 5′-GGGAAATCGTGCGTGACATCAAAG-3′ and antisense 5′-CATACCCAAGAAGGAAGGCTGGAA-3′. For all PCRs, standard curves, dissociation curves, and migration of PCR products on acrylamide gels were done to confirm the specificity of the products. Moreover, two PCRs were performed as negative controls: one without cDNA template, and the other using reverse transcription reaction that never received SuperScript II reverse transcriptase enzyme. Results were estimated as C_t values, and the fold change of the expression of target gene in DU145 compared with 4-2 cells was expressed as $2^{\Delta\Delta Ct}$. The ΔC_t was obtained from the subtraction of the mean C_t for the target with the mean C_t for the internal control gene (*β-actin*). The $\Delta\Delta C_t$ is the mean difference between the ΔC_t obtained from DU145 RNA extracts minus ΔC_t obtained from 4-2 RNA extracts. All PCRs were repeated twice for each set of primers.

Conditioned Growth Medium Preparation

Four 10-cm plates were seeded with 1.0×10^6 cells (DU145 or 4-2 cells) in complete growth media. The next day, the cells were washed twice with PBS, and the growth medium was replaced with 5 ml of serum-free RPMI for 1 hour. The conditioned media were collected, filtered through 0.45-μm Acrodisc syringe filter units (Pall Corporation, Ville St. Laurent, Quebec, Canada), and kept on ice. The filtrates were concentrated to a final volume of 350 μl with Amicon Ultra centrifugal filter devices with a 3-kDa molecular weight cutoff (Millipore, Bedford, MA). Fresh RPMI was treated the same way as a control for cell experiments.

MTT Proliferation Assay

The cell proliferation was measured by the colorimetric MTT assay (thiazolyl blue tetrazolium bromide; Sigma-Aldrich, Oakville, Ontario, Canada). Briefly, cells were seeded in 96-well plates (BD Biosciences, Mississauga, Ontario, Canada) in triplicate with 100 μl of a 5.0×10^4-cells/ml cell suspension in complete growth medium. The following day, cells were carefully washed twice with PBS twice and were incubated with 50 μl of either fresh RPMI, concentrated RPMI, DU145 or 4-2 concentrated conditioned growth media (DU145 and 4-2 CM, respectively). After 48 hours, 12.5 μl of an MTT solution (5 mg/ml in PBS) was added to each well for 4.5 hours at 37°C/5% CO_2. The medium was then carefully discarded, and the cells were solubilized with 100 μl of isopropanol/0.04N HCl solution. The absorbance was measured at a wavelength of 550 nm with a reference at 650 nm in microplate reader (SpectraMax190; Molecular Devices, Sunnyvale, CA).

Cell Count Assay

Cells were plated at a density of 5.0×10^4/well in six-well plates (BD Biosciences) in duplicates. Complete growth medium was changed after 48 hours. After incubation, cells were washed in PBS, trypsinized, and counted after staining in 0.4% (wt/vol) trypan blue solution (Sigma-Aldrich). Only viable cells were counted in duplicate.

Colony Formation Assay

Cell lines were seeded in six-well plates (BD Biosciences) at a density of 300 cells/well in triplicate. Cells were maintained in complete growth medium for 10 days. After colony formation, medium was discarded, and cells were washed once with PBS. Colonies were fixed and stained in 5 mg/ml methylene blue/50% methanol solution for 10 minutes. Excess of staining solution was removed carefully with distilled water and the plates were dried overnight before scanning with Li-Cor Odyssey Infrared Imaging System (Li-Cor Biosciences, Lincoln, NE). Scanned images were analyzed with ImageJ software 1.37v (http://rsb.info.nih.gov/ij/) to measure the total particle area.

Flow Cytometric Analysis of Apoptosis without Cell Fixation

Propidium iodide DNA staining. Cell lines were seeded in 10-cm plates (5.0×10^5 cells) in complete growth media and grown overnight. Afterwards, cells were washed three times with PBS, incubated in fresh complete growth medium for 12 hours, and harvested with

trypsin (including the supernatant). The cell pellets were washed once with PBS, centrifuged, and resuspended in 50 µl of PBS. A chromatin decondensation treatment was performed using 450 µl of H-buffer/Triton X-100 (20 mM HEPES, pH 7.2, 0.16 M NaCl, 1 mM EGTA, and 0.05% Triton X-100) warmed at 37°C for 1 minute on ice. After this incubation, cells were gently centrifuged for 5 minutes and 450 µl of the supernatant was discarded. Cell pellets were then gently resuspended with the remaining supernatant, and the DNA staining was performed using 450 µl of H buffer containing 10 µg/ml of RNAseA (Sigma-Aldrich) and 10 µg/ml of propidium iodide (PI) (Sigma-Aldrich) for 30 minutes at room temperature in the dark.

Fluorescence-activated cell sorter analysis. After the PI staining, cells were analyzed on a FACScan cytometer (BD Biosciences). Forward and side scatter signals were used to establish the live gate to exclude debris and cell clumps. A minimum of 10,000 gated events by sample were acquired. The fluorescence of PI was collected in red channel on a linear scale (FL3). A second live gate was set using the FL3-A and FL3-W parameters of the doublet discrimination module, allowing single cell measurements. Fluorescence intensity distribution was analyzed with the CellQuest software (BD Biosciences), whereas the distribution of nonapoptotic cells into the phases of the cell cycle was determined using the ModFit software (Verify Software House, Topsham, ME).

Human Tumor Xenograft Models

Four-week-old female athymic nude mice (*nu/nu*; Charles River Laboratories, Wilmington, MA) were inoculated subcutaneously at the opposite sides of the flank with 3.0×10^6 cells per inoculum (five mice/group). Cells were grown in complete media and harvested at their exponential growing state. Mice were housed under pathogen-free conditions, and the implantations were done under anesthesia conditions in laminar flow hood. Xenografts were measured three times per week, and volume (V) was determined by this equation: $V = (L \times W^2) \times 0.5$, where L is the length and W is the width of the xenograft.

Immunohistochemistry

Subcutaneous tumors derived from DU145 and 4-2 cell lines were eradicated, formalin-fixed, and paraffin-embedded. Immunohistochemical staining was carried out on 3-µm sections by the Ventana NexES autostainer with the enzyme-labeled biotin-streptavidin system and the solvent-resistant DAB Map detection kit (Ventana Medical System, Tucson, AZ) using either p53 (1:200), MUC1 (epithelial membrane antigen; 1:200) or CDK4 (cyclin-dependent kinase 4; 1:100) anti–human monoclonal antibodies or prostate-specific antigen (PSA; 1:10,000) anti–human polyclonal antibody (Dako Canada, Burlington, Ontario, Canada; Thermo Fisher Scientific, Fremont, CA). The slides were counterstained with hematoxylin. The images were acquired using an Axioskop 2 phase-contrast microscope (Carl Zeiss, Thornwood, NY) and processed using Image Pro software (Media Cybernetics, Bethesda, MD).

Mass Spectrometry Analysis of Conditioned Media

Sample preparation. The DU145 and 4-2 conditioned growth media were prepared as described earlier in this section, except that the concentrated media were washed in centrifugal filter device with 12 ml of water before being collected and lyophilized. The samples were then solubilized with 100 µl of acidified water–0.1% trifluoroacetic acid. Acetone precipitation was performed with a ratio 4:1 (vol/vol). After a centrifugation at 13,000 rpm at 4°C for 30 minutes, pellets were solubilized in 50 mM pH 8.0 ammonium bicarbonate (NH_4HCO_3), a reduction of cysteine residues with a 45-mM dithiothreitol solution was performed for 15 minutes at 50°C, and a subsequent alkylation was performed with a 100-mM iodoacetamide solution for 15 minutes at room temperature in the dark.

Trypsin digestion. The samples were placed on ice for 30 minutes in 50 µl of proteases solution (sequence grade-modified trypsin [Promega] at 0.02 mg/ml in 25 mM NH_4HCO_3). Digestions were performed overnight at 37°C. The samples were then desalted and concentrated using C18 ZipTips (Millipore) before mass spectrometry analyses.

Matrix-assisted laser desorption/ionization tandem time-of-flight (MALDI-TOF/TOF) analyses. The MALDI TOF/TOF mass spectrometer (Ultraflex II; Bruker Daltonik, Bremen, Germany) used in this study was equipped with an Nd:YAG laser (355 nm) with a repetition rate of 200 Hz. Mass spectra were the sums of 8000 shots acquired in positive ion reflectron TOF mode. The acceleration potential was 25 kV. For MS^2 analysis, 2000 shots were acquired for parent ion selection and 10,000 shots for fragments selection. For MALDI analysis, the matrix used was α-cyano-4-hydroxycinnamic acid ACN: H_2O/trifluoroacetic acid 0.1% (7:3). Calibration was performed with peptides calibration standard (Bruker Daltonik). Samples underwent software processing with FlexAnalysis 2.4 and Biotools 2.2 (Bruker Daltonik) for baseline subtraction and peaks detection.

Protein identification. Protein identification was performed under the MASCOT sequence query search program using the SwissProt database filtered for the taxonomy *Homo sapiens*. A tolerance of 1 Da for peptide and 0.6 Da for tandem mass spectrometry (MS/MS) was set. Only protein sequences with a MOWSE score higher than 36 (indicating significant homology or identity) and identified in several samples representing at least two significant MS/MS were considered. Methionine oxidation and acetylation of N-terminals were defined as variable modification.

Statistical Analyses

All experiments were repeated at least three times, except for human tumor xenografts and microarray analysis. Comparisons between the test group and controls of this study were done using Student's t test.

Results

PACE4 Expression in Clinically Localized Prostate Tumors

We tested the expression of PCs in 47 primary prostate tumor samples obtained from patients undergoing surgery. The majority of the patients (i.e., $n = 34$) had clinically localized tumors and 13 had hormone-refractory recurrent prostate carcinoma. All collected samples were subjected to histopathologic examination. Only tissues where all epithelial cells were neoplastic were dissected and used for further studies. Real-time PCR was used to evaluate PACE4, furin, and PC7 mRNA expression levels in prostate tumor tissues using nine

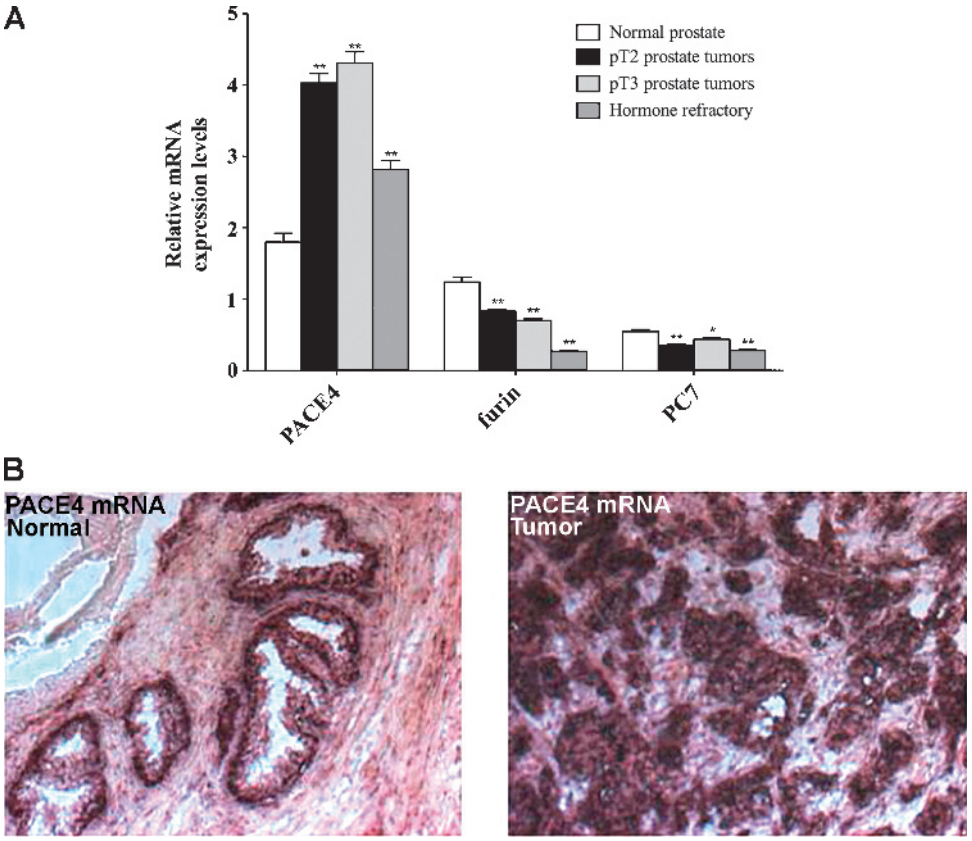

Figure 1. Relative mRNA expression levels of PCs in normal and tumoral prostate tissues. (A) Real-time PCRs from tissue specimens were performed with PACE4, furin, PC7, and PPIA specific primers. Nine normal prostate tissues and 47 prostate tumors (separated into three groups) were used for the comparative analyses. Clinical stage classification of prostate tumors, based on TNM system, was as follows: pT2, tumors strictly confined to the organ (18 samples); and pT3, tumors with extracapsular extensions (16 samples). Hormone-refractory prostate tumor tissues (13 samples) were issued from patients who relapsed after receiving endocrine therapy. Values are mean ± SEM. *$P < .05$, **$P < .001$. (B) PACE4 *in situ* hybridization in epithelial cells from normal and tumoral prostate tissues (arrows indicate purple staining corresponding to PACE4 mRNA).

matched normal prostate tissues as a reference (Figure 1*A*). The tissues were grouped into similar clinical stages based on TNM system as 18 pT2 samples (tumors strictly confined to the organ), 16 pT3 samples (tumors with extracapsular extension), and 13 hormone-refractory samples (tumors no longer responsive to endocrine therapy). The mean relative PACE4 mRNA expression levels (Figure 1*A*) were significantly higher for all cancer groups (pT2, 4.0 ± 0.1; pT3, 4.3 ± 0.2; and hormone refractory, 2.8 ± 0.1), when compared with the mean level found in normal prostate tissues (1.8 ± 0.1). Real-time PCR for the other PCs showed that furin, PACE4, and PC7 were the most expressed PCs in normal prostate tissues. However, only PACE4 mRNA expression increased in tumor tissues, whereas the others showed a generalized reduction in cancer tissues. This higher PACE4 expression, particularly in epithelial cells, was directly assessed

Table 1. PACE4 Is Upregulated in Prostate Cancer according to Oncomine Database*.

Study	Description	Fold Change	*P*	Number of Measured Genes	Overexpression Gene Rank	Reference
1	Prostate carcinoma (n = 8) *vs* prostate gland (n = 4)	1.951	1.58*e* − 4	4564	7 (in top 1%)	*Cancer Res.* 2001;61(15):5692–5696
2	Prostate carcinoma (n = 61) *vs* prostate gland (n = 39)	2.190	9.12*e* − 15	10,021	35 (in top 1%)	*Proc Natl Acad Sci USA.* 2004;101(3):811–816
3	Prostate carcinoma (n = 65) *vs* prostate gland (n = 23)	1.246	4.65*e* − 7	7820	89 (in top 2%)	*J Clin Oncol.* 2004;22(14):2790–2799
4	Prostate carcinoma (n = 44) *vs* prostate gland (n = 13)	1.271	7.56*e* − 5	12,427	113 (in top 1%)	*Cancer Res.* 2006;66(8):4011–4019
5	Prostate carcinoma (n = 7) *vs* prostate gland (n = 6)	2.627	5.93*e* − 4	19,079	250 (in top 2%)	*Cancer Cell.* 2005;8(5):393–406
6	Prostate adenocarcinoma (n = 27) *vs* prostate gland (n = 8)	1.349	5.30*e* − 4	17,358	1202 (in top 7%)	*Cancer Res.* 2003;63(14):3877–3882

*Available at: http://www.oncomine.org.

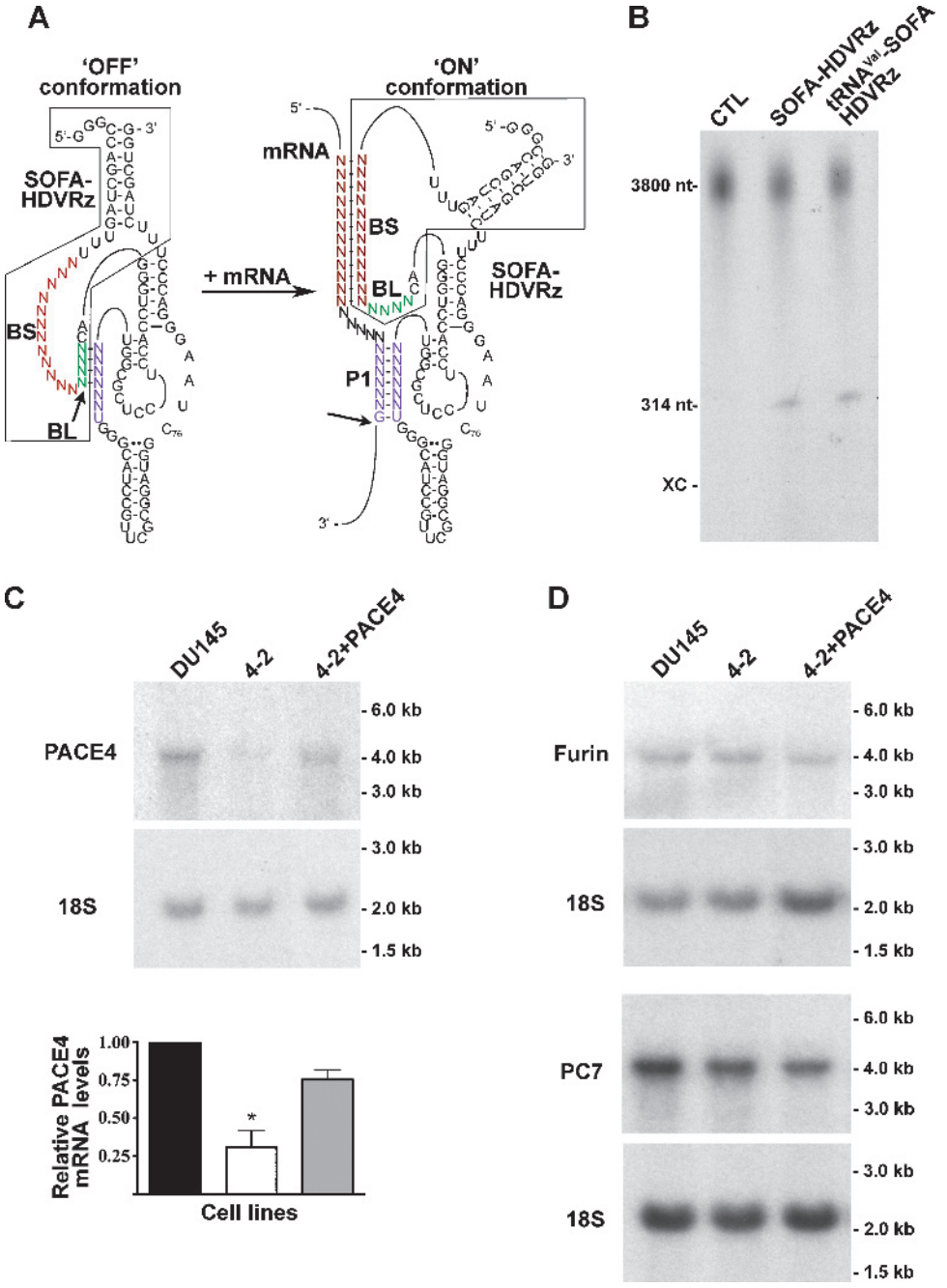

Figure 2. Down-regulation of PACE4 expression in DU145 cells. (A) The secondary structure of both the "OFF" and "ON" conformation of the SOFA module (box) attached to the classic HDVRz. The biosensor (in red, BS) and the blocker (in green, BL) can be modified to be hybridized on a specific mRNA target (N indicates A, C, G, or U). After the recognition of the mRNA, the P1 stem (in purple, P1) issued from the sequence-specific hybridization of the HDVRz with the targeted RNA will allow the catalytic cleavage of the latter, as indicated by the arrow. (B) Autoradiogram of *in vitro* cleavage assays performed with either the SOFA-HDVRz or the chimeric RNA transcript $tRNA^{Val}$-SOFA-HDVRz both specific for PACE4 RNA. The control lane is the migration of the internally ^{32}P-radiolabeled 3800 nt PACE4 RNA alone. The BS, BL, and P1 nucleotide sequences of the PACE4-SOFA-HDVRz used are indicated in the Materials and Methods section. XC indicates the position of xylene cyanol after migration on the denaturing 5% PAGE gel. (C and D) Autoradiograms of Northern blot hybridizations showing levels of PACE4 (C), furin (D), and PC7 (D) mRNA in untransfected DU145 cells (control cell line) or in cell lines either transfected with the expression vector coding for the $tRNA^{Val}$-PACE4-SOFA-HDVRz alone (4-2) or cotransfected with a PACE4 cDNA expression vector (4-2 + PACE4) are shown. The bands corresponding to the 18S ribosomal RNA are shown for all blots. The size markers are shown on the right. The expression levels of PACE4 mRNA in transfected cell lines relative to the unstransfected DU145 cells were obtained by densitometric analyses using 18S ribosomal RNA as loading control (C). Values are mean ± SEM ($n = 3$). *$P < .05$.

by an *in situ* hydridization. Normal prostate tissues showed the expected epithelial cell distribution of PACE4 mRNA. However, tumors showed disorganization of the tissue structure, with a higher PACE4 expression and even cells invading the stroma (Figure 1*B*).

Because PACE4 was the only member of the PC family to be overexpressed in prostate tissues, we investigated its expression levels in the Oncomine database (http://www.oncomine.org). As summarized in the Table 1, six independent studies reported a significant

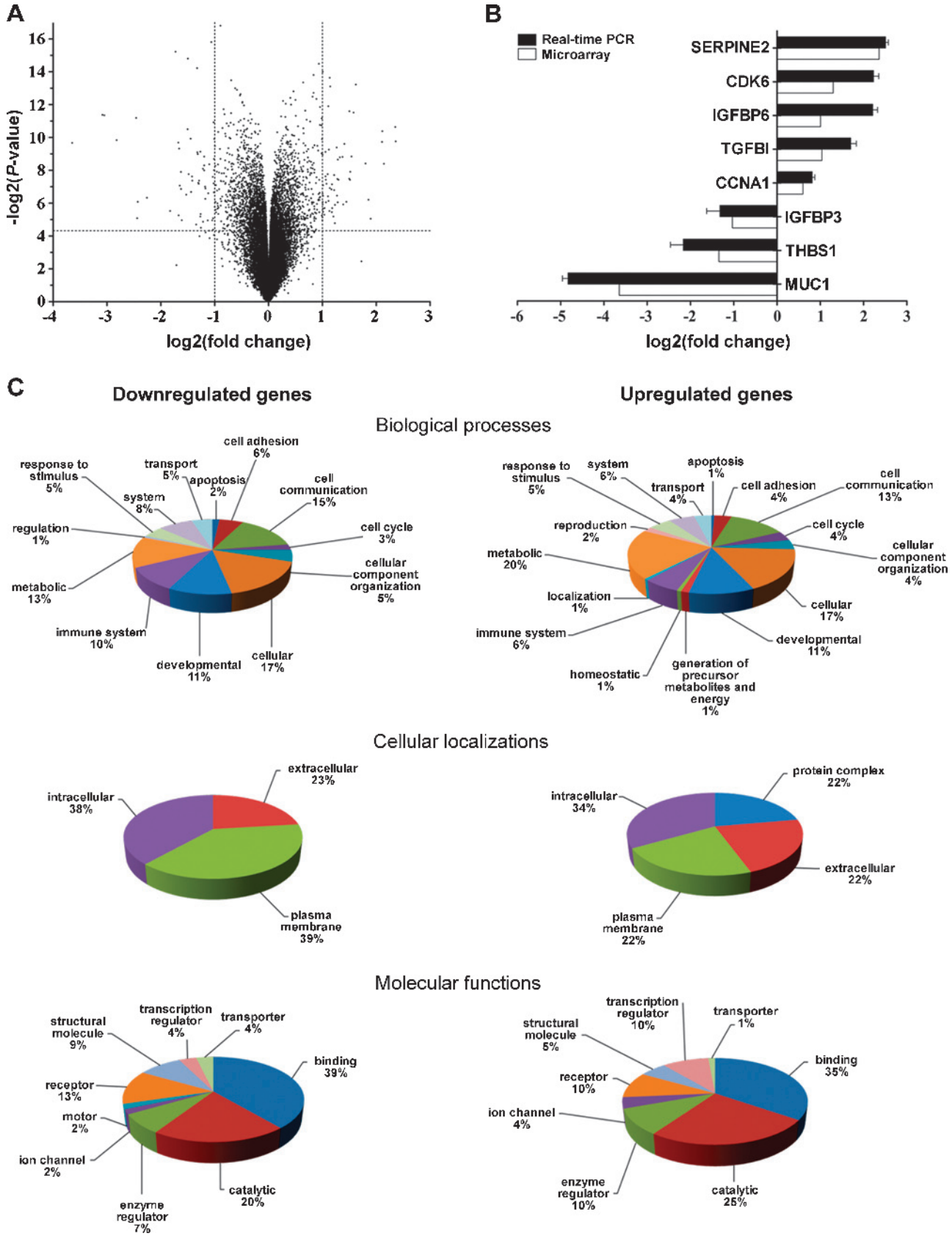

overexpression of PACE4 ($P < .001$) in prostate cancer tissues compared with corresponding normal tissues. Moreover, in five of the six studies, the PACE4 overexpression rank was within the top 2%, whereas the remaining was in the top 7%. It is noteworthy to report that furin, PC5/6, and PC7 did not show an up-regulation of their expression within those studies. These microarray studies, combined with our real-time PCR results, strongly suggest that PACE4 is associated with prostate cancer (i.e., potential biomarker or therapeutic target). Although these studies only measured PCs mRNA expression levels in prostate cancer tissues and not their enzymatic activity, we still decided to focus on PACE4 for this study.

Rational Design of SOFA-HDVRz Targeting PACE4 mRNA

SOFA-HDVRz as a gene silencing tool. Considering the high expression level of PACE4 mRNA in tumoral prostate tissues, we decided to evaluate the contribution of this enzyme to the maintenance of the tumorigenic state *in vitro* and *in vivo*. Because there are no PACE4-specific and potent inhibitors available [9,46], we opted for a highly specific molecular approach targeting PACE4 mRNA. We previously showed that hepatitis delta virus ribozyme (HDVRz) could be a powerful and specific silencing tool in cultured cells [40]. Here, we tested a new generation of HDVRz harboring a switch on/off adapter (SOFA-HDVRz), resulting in an enhanced *in vitro* specificity and potency [47,48]. As shown in Figure 2*A*, the SOFA-HDVRz has three new features over the classic HDVRz. First, a blocker stem of 4 nt prevents the formation of the P1 stem, essential for the cleavage event. A biosensor of 12 nt at the 5′ end of the blocker stem compels the SOFA-HDVRz to maintain an inactive state ("OFF" conformation) until the right complementary RNA hybridizes. This sequence-specific hybridization releases the P1 stem from the blocker, allowing the formation of the P1 stem.

SOFA-HDVRz design. We used the complete sequence of human PACE4 cDNA (GenBank database accession number M80482) to design a selective SOFA-HDVRz against PACE4 mRNA. The bioinformatics analysis of the selected sequence reveals no other matches in the entire genome than that of PACE4. The exquisite specificity of the SOFA ribozyme approach has been validated [49]. Figure 2*B* shows the *in vitro* cleavage of PACE RNA with a selected PACE4-SOFA-HDVRz cleaving into the prodomain coding sequence of the transcript at position 519. As shown on the autoradiogram of the PAGE gel, the reaction generated only one cleavage product that could be seen after the addition of the PACE4-SOFA-HDVRz. To confirm the specificity of this molecule, we firstly tested the same ribozyme against a radiolabeled human furin transcript, and secondly, we used a catalytically inactive mutant (C76A) of the SOFA-PACE4-HDVRz against the PACE4 transcript [47]. In both cases, no cleavage product could be observed, confirming the capacity of the PACE4-SOFA-HDVRz to selectively cleave its target *in vitro*.

Down-regulation of PACE4 mRNA in DU145 Cells

Expression vector. We used an expression vector containing the $tRNA^{Val}$ promoter to produce the PACE4-SOFA-HDVRz into transfected cells [40]. To insure that the $tRNA^{Val}$ part did not interfere with the catalytic activity of the associated SOFA-HDVRz, we performed an *in vitro* cleavage assay by incubating the chimeric transcript ($tRNA^{Val}$-SOFA-HDVRz) with an internally radiolabeled PACE4 RNA (Figure 2*B*). As seen on the autoradiogram of the PAGE gel, the addition of the $tRNA^{Val}$ motif did not modify neither the specificity nor the level of the cleavage activity of the PACE4-SOFA-HDVRz.

Northern blots. We transfected the PACE4-SOFA-HDVRz expression vector (named $ptRNA^{Val}$-PACE4-SOFA-HDVRz) into DU145, a highly invasive, androgen-independent prostate epithelial tumor cell line. These cells were chosen for their high level of PACE4 expression, aggressiveness, and ease of transfection when compared with the androgen-dependent LNCaP or the androgen-independent PC-3 cells. Stable cell lines transfected were established by the selection of clones resistant to hygromycin B. Northern blot analyses on total RNA extracts were performed for wild-type DU145 (DU145), DU145 transfected with $ptRNA^{Val}$-PACE4-SOFA-HDVRz (cell line 4-2), and 4-2 + PACE4 cells, which are 4-2 cell lines cotransfected with the PACE4 cDNA expression vector. As seen in Figure 2*C*, the PACE4 mRNA expression level in the SOFA-HDVRz transfected cell line was significantly reduced when compared with the untransfected cells. These levels were partially reestablished by the overexpression of PACE4 cDNA. The graph shows a densitometric analysis using 18S ribosomal RNA as loading control performed to quantify the mRNA expression levels in these clonal cell lines using wild type DU145 cells as reference (0.3 ± 0.1 and 0.75 ± 0.06 for 4-2 and 4-2 + PACE4, respectively). The mRNA expression levels of two other endogenous PCs confirmed the specificity of the PACE4-SOFA-HDVRz cleavage. Levels of furin and PC7 mRNA (Figure 2*D*) remained unchanged in the 4-2 cells, confirming the reduction of PACE4 expression without affecting the expression of other endogenous PCs. Because the autoradiograms suggested a slight variation in the expression of these two mRNA in the 4-2 + PACE4 cell line, we further examined these cell lines by quantitative PCR, confirming that no significant differences are observed.

Gene Expression Profiling in DU145 Cells

With the aim of better understanding the general contribution of PACE4 on prostate cancer growth, we performed a comparative gene

Figure 3. Microarray analysis and real-time PCR. (A) Volcano plot of differentially expressed genes in DU145 *versus* 4-2 cells measured with Illumina human expression bead chips. Vertical dashed lines show thresholds values for the fold change, whereas the horizontal dashed line indicates the threshold value for the *P* value (.05). Only genes with *P* values higher than the threshold with a $\log_2$(fold change) lower than −1 or higher than 1 were include in Tables W1 and W2, respectively. (B) Confirmation of values obtained with microarrays by real-time PCR. Amplification and detection of cDNA were performed using SYBR Green I dye. The expression levels, measured by real-time PCR (black bars), were normalized using *β-actin* as internal control. The white bars indicate values obtained from microarray analyses. (C) Classification of differentially expressed genes in 4-2 cells compared with DU145 according to their biologic processes, cellular localizations, and molecular functions. The PANTHER classification system (http://www.pantherdb.org) had no attributed gene ontology grouping for nine downregulated genes and six upregulated genes.

expression analysis by DNA microarray screening with DU145 and 4-2 cells (Figure 3*A*). The gene expression levels measured by microarrays were validated by real-time PCR for eight genes covering a broad range of fold changes (Figure 3*B*). For all the genes tested, the quantitative PCR results (black bars) were either similar or higher than microarray data, confirming that microarray results (white bars) were reliable or even underestimated, at least for those tested. Of the 38,275 genes tested, 59 genes (0.15%) showed a two-fold decrease, whereas 62 genes (0.16%) had a two-fold increase in 4-2 cells ($P < .05$). These genes correspond to the dots found in the higher left and right quadrants of the volcano plot, respectively (Figure 3*A*; Tables W1 and W2).

The PANTHER (Protein Analysis THrough Evolutionary Relationships; http://www.pantherdb.org) system was used to group the gene listed in Tables W1 and W2 according to their biologic processes, cellular localizations, and molecular functions using the gene ontology classification (Figure 3*C*). Among the 59 downregulated and 62 upregulated genes, some could not be associated with any group into the database (9 and 6, respectively), whereas the others were distributed among multiple categories in comparable proportions between the two set of genes. Genes associated to cell communication, cellular processes (including cell cycle, cell growth, cell motion, and cell proliferation–associated genes), developmental, and metabolic processes are part of the major biologic functions affected by PACE4 down-regulation. The analysis of the cellular localization suggests a central role of PACE4 into the processing of various intracellular, membrane-bound, protein complexes and extracellular proteins. Finally, the major molecular functions affected by PACE4 down-regulation in 4-2 cells include cellular binding, transcription regulator, and catalytic (enzymatic) activity.

Although many of the listed genes have known biologic functions, not all proteins encoded by these genes are known or potential PACE4 substrates. Some interesting possibilities were observed, such as the analysis of CDH1 amino acid sequence (i.e., a cadherin) revealed that it is a potential PACE4 substrate because it necessitates a proteolytic processing event at the $_{149}$LRRQKR↓DW$_{156}$ site of its propeptide domain to become biologically active [50]. Moreover, PTHLH also carries a potential PACE4 processing site at the $_{31}$SRRLKR↓AV$_{38}$ of its propeptide region [51]. However, it is not excluded that downregulated genes (e.g., *MUC1*, a known prostate cancer oncoprotein [52]) might be indirectly affected by PACE4 expression levels without being a direct substrate harboring a PC processing [53].

PACE4 Is Important for the Activity of Growth Factors

Considering the previous links established between PCs expression, growth factors, and tumor progression, we measured cell proliferation activity by generating concentrated conditioned media issued from either untransfected DU145 or the 4-2 cell line. These growth media were incubated with DU145 cells for 48 hours, and proliferation state was measured by adding the MTT compound. As shown in Figure 4*A*, concentrated conditioned growth medium issued from DU145 cells (DU145 CM) stimulated the proliferation of DU145 cells in a similar range than the complete growth medium RPMI + FBS did ($OD_{550nm} - OD_{650nm}$ = 0.44 ± 0.02 and 0.40 ± 0.02, respectively). This higher proliferation was not measured in cells incubated with conditioned growth medium issued from the 4-2 cell line (4-2 CM), where the $OD_{550nm} - OD_{650nm}$ value (0.31 ± 0.02) was similar to that obtained with cells incubated with either RPMI or concentrated RPMI treated in

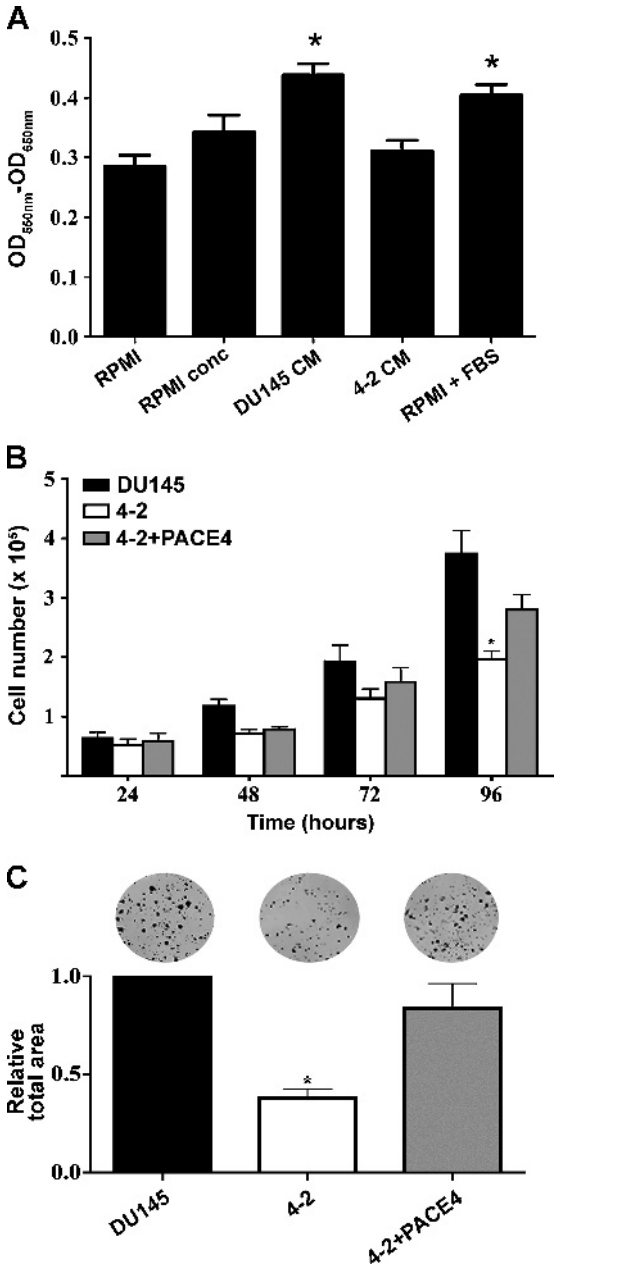

Figure 4. Proliferation of DU145 cells with reduced PACE4 expression. (A) MTT proliferation assay with conditioned media. DU145 cells (5.0×10^3/well in triplicate) were incubated either with RPMI, concentrated RPMI (RPMI conc), DU145 conditioned medium (DU145 CM), or 4-2 CM for 48 hours. After treatment, MTT solution was added for 4.5 hours, and $OD_{550nm} - OD_{650nm}$ of solubilized cells was measured and compared using untreated cells (RPMI) as reference. Values are mean ± SEM ($n = 7$). (B) Time-dependent proliferation of untransfected DU145 cells (DU145) or expressing $tRNA^{Val}$-PACE4-SOFA-HDVRz with or without partially reestablished PACE4 expression (4-2 and 4-2 + PACE4, respectively) was assessed by counting total cell number after 24, 48, 72, and 96 hours of incubation time. Values are mean ± SEM ($n = 3$). (C) Colony formation after 10 days of incubation of DU145, 4-2, and 4-2 + PACE4 cell lines. Culture plates with fixed and stained cells were scanned, and the total particle area was measured. Typical result is illustrated for each cell line above in the upper part of the panel. The relative total area of the transfected cell lines compared with the control cell line is shown. Values are mean ± SEM ($n = 9$ for DU145 and 4-2 + PACE4 and $n = 7$ for 4-2). *$P < .05$.

the same way than the concentrated conditioned media, i.e., 0.28 ± 0.02 and 0.34 ± 0.03, respectively. Thus, these results suggest that PACE4 is important for the activity of growth factors that maintain a high proliferative status.

PACE4 Down-regulation Slows DU145 Proliferation In Vitro

To further characterize the cell proliferation reduction observed with conditioned media experiments, we counted the total cell number of our stable cell lines at different times. As seen in Figure 4*B*, the results showed a significant reduction of proliferation for the 4-2 cell line (≈200,000 ± 10,000 cells) when compared with untransfected DU145 (≈380,000 ± 40,000 cells) 96 hours after the initial plating. It should be noted that these cell count experiments were carried out in the presence of complete growth media, which includes FBS; otherwise, the 4-2 cell line is very difficult to maintain and cell counts could not be obtained at the 72- and 96-hour time points. The observed reduced cell counts were partially reversed in the cell line 4-2 + PACE4 (≈280,000 ± 30,000 cells). We also performed an *in vitro* clonogenic assay on the same cell lines to detect the proportion of cells that retained the capacity to form colonies (Figure 4*C*). The results of this assay correlate the proliferation of DU145 with PACE4 expression levels, as we observed a 68% reduction of the colony growth in 4-2 cells when compared with wild-type DU145, whereas this colony formation capacity was partially restored in 4-2 + PACE4 cells (16% reduction when compared with the same cells).

PACE4 Inhibition Prevents Tumor Growth in Xenograft Tumor Model

We tested the ability of our experimental cell lines to grow as tumors in the nude mouse model. We injected 3×10^6 cells subcutaneously in nude mice flanks and measured tumor volumes 1 week after injection. As shown in Figure 5*A*, the reduction of PACE4 mRNA expression level reduced dramatically the ability of the 4-2 cell line to induce tumor growth, whereas untransfected DU145 cells were able to develop into well-defined tumor masses. After 31 days, subcutaneous tumors were removed from nude mice for immunohistochemical staining of p53, MUC1, CDK4, and PSA proteins. We used p53 as a marker of tumoral cells because DU145 cells strongly express a double-mutant inactive form of this protein [54]. As shown in Figure 5 (*B* and *C*), the tumor derived from the 4-2 cell line contained a much lower number of tumoral cells when compared with the tumor derived from the DU145 cell line. We confirmed that the PSA protein was not expressed [55], and it was therefore included as a negative control (Figure 5, *H* and *I*). As suggested by the comparative gene expression analysis of DU145 and 4-2 cell lines, the 4-2 tumor showed a lower expression of the oncogene MUC1 than those found in the DU145 tumor (Figure 5, *D* and *E*). Finally, the staining for the CDK4 protein, a cell cycle activator, was drastically lower in the 4-2 tumor when compared with the DU145 tumor (Figure 5, *F* and *G*), which is in agreement with the lower proliferation rates of the 4-2 cell line described earlier (Figure 4).

Lower PACE4 Expression Induces Apoptosis in the 4-2 Cell Line

Because PACE4 expression correlated with the reduced cell proliferation of DU145 cells, we decided to analyze the cell cycle of DU145, 4-2, and 4-2 + PACE4 cells by flow cytometric analysis using the PI staining. As shown in Figure 6*A*, the proportion of hypodiploid cells (characteristic of apoptotic cells) is higher in the 4-2 cell line (12.3%)

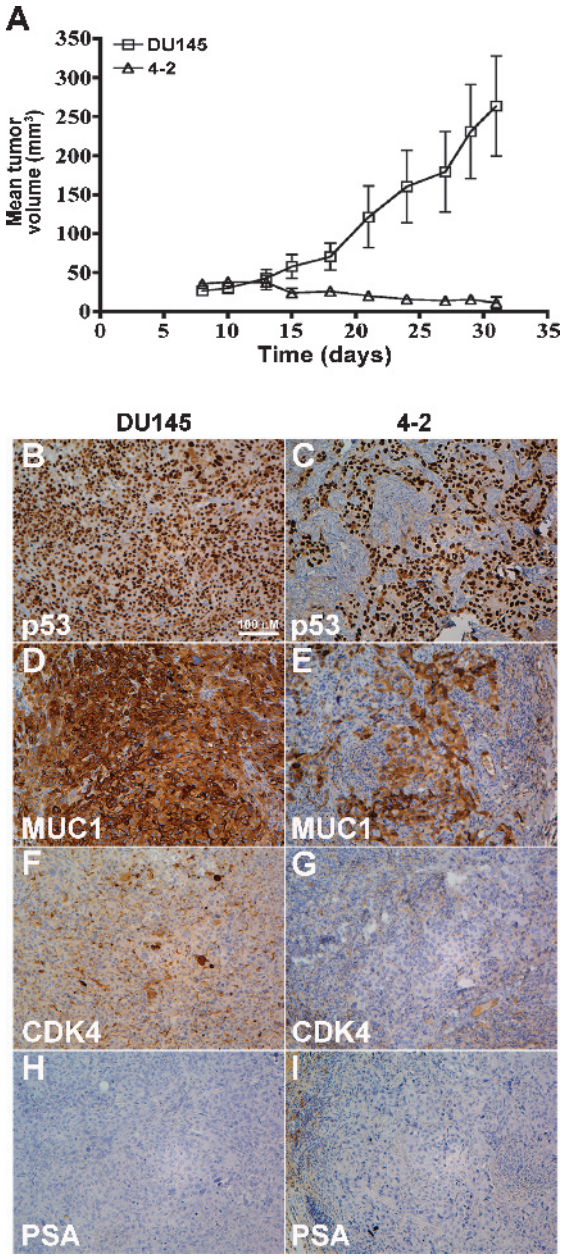

Figure 5. *In vivo* tumorigenicity assay and immunohistochemistry. (A) 3.0×10^6 DU145 and 4-2 cells were subcutaneously injected in 4-week-old *nu/nu* female mice (two injections/mice, five mice/group). The length and the width of the tumors were measured three times per week for 31 days. Values shown are mean ± SEM of tumors volumes for all tumors measured per mice group. Immunohistochemical staining of tumors derived from DU145 and 4-2 cell lines for p53 (B, C), MUC1 (D, E), CDK4 (F, G), and PSA (H, I) proteins. All images were acquired at the same magnification (100×).

than those found either in DU145 or in 4-2 + PACE4 cells (1.74% and 3.30%, respectively). Moreover, 78.8% of the nonapoptotic 4-2 cells were blocked into the G_0/G_1 phase of the cell cycle, and only 3.84% were into the G_2-M phase. This is in contrast with the DU145 cells, where only 67.3% of nonapoptotic cells were in the G_0-G_1 phase, and 14.5% entered into the G_2-M phase. However, 14.5% of the latest cells are in the G_2-M phase, whereas only 3.84% of 4-2 cells are distributed in this phase. Thus, the lower cell proliferation observed in the 4-2 cell line can be attributed to a higher apoptosis rate

and a blockade into the G_0-G_1 phase of the cell cycle. Interestingly, the study of the partial rescue cell line 4-2 + PACE4 showed that a lower population of these cells were in apoptosis when compared with the 4-2 cells (3.30% and 12.3%, respectively), confirming an important role of PACE4. However, these cells with a partially restored PACE4 expression still seemed to be blocked into the G_0/G_1 phase of cell cycle as for the 4-2 cells (80.6% and 78.8%, respectively) and like 4-2 cells, the 4-2 + PACE4 cells had a low percentage of cells into the G_2-M phase (3.61%). Thus, the partial reestablishment of PACE4 expression levels leads to a lower apoptotic percentage of DU145 cells but still results in a partial blockade of the cell cycle into the G_0/G_1 phase.

Because important differences were observed between DU145 and 4-2 cell lines in regard to apoptosis, we sought potential effects on proapoptotic factors (Figure 6*B*). On the type of analysis, we used DU145 and 4-2 cell line CM digested with trypsin to perform a MALDI-TOF/TOF analysis. One marker of interest was identified at a mass of 1227.8 Da only in the 4-2 CM. The protein identification was then performed under the MASCOT sequence query search program

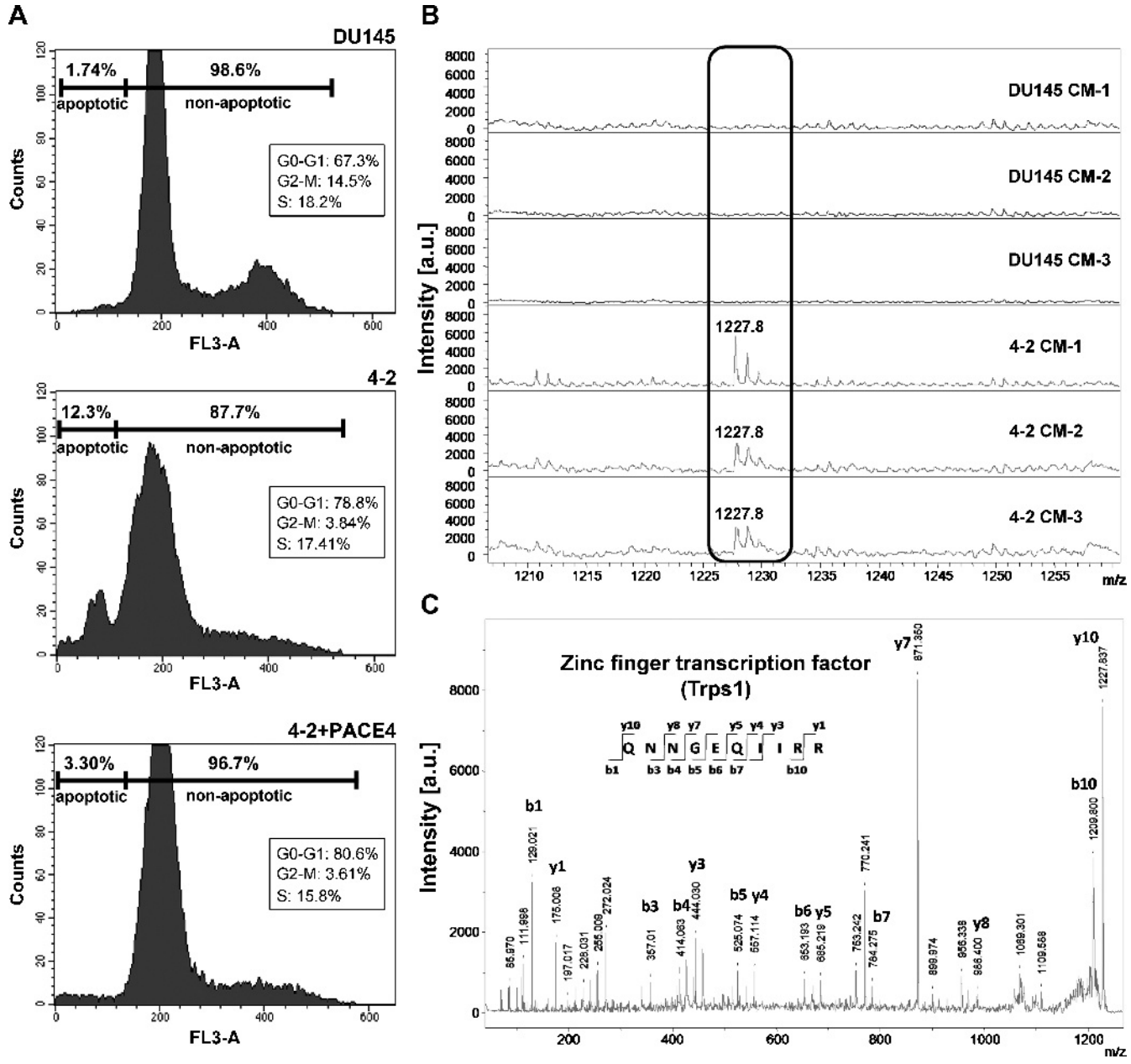

Figure 6. Cell cycle analysis and identification of an apoptotic biomarker by MALDI-TOF/TOF. (A) DNA content of DU145, 4-2 and 4-2 + PACE4 cells was determined by flow cytometric analysis using PI staining without cell fixation. The 4-2 cells showed a higher level of fragmented DNA than DU145 and 4-2 + PACE4 cells (12.30%, 1.74%, and 3.30%, respectively), indicating a higher population of hypodiploid cells for the 4-2 cell line, a characteristic of apoptotic cells. Inserts show the distribution of nonapoptotic cells into the phases of cell cycle. (B and C) Detection and identification of the apoptotic biomarker TRPS1 were done by MALDI-TOF/TOF in positive reflectron mode from different secretomes coming from triplicates of DU145 and 4-2 conditioned culture media after trypsin digestions. B represents the mass spectra comparison between conditioned media from both cell lines and the box shows a biomarker with a m/z of 1228 in 4-2 CM. C shows the identification by fragmentation of this peak as the zinc finger transcription factor TRPS1 by MALDI-TOF/TOF.

(Figure 6*B*). This biomarker corresponded to a fragment of the TRPS1 transcription factor, a protein issued from the apoptosis-associated gene *GC79/TRPS1* that encodes an atypical multitype zinc finger GATA-type transcription factor associated to prostate cancer that potently and specifically represses transcriptional activation mediated by other GATA factors [56,57]. Although there is no evidence for the secreted release of TRPS1 or of a possible isoform, we might conclude that its detection in CM is the result of increased apoptosis in the 4-2 cell line.

Discussion

The relationship between PCs and cancer has become stronger within the last few years. However, because cancer cell lines generally coexpress multiple PCs, it still remains unclear if only one or multiple PCs are more important in cancer progression. In this study, we chose to focus on PACE4 because of our finding that this PC is specifically overexpressed in different clinical stages of prostate cancer tissues, arguing for a particular role of PACE4 in the establishment or the maintenance of prostate cancer (Figure 1). To reinforce our findings in human prostate cancer tissues, we also evaluated six independent studies that also report the selective PACE4 overexpression in prostate cancer (Table 1), confirming the potential importance of this enzyme to sustain the disease.

There are various ways in which we could choose to study the role of PACE4 in prostate cancer. Molecular and pharmacological inhibitions have particular advantages, as long as they can be shown to be specific. At the present time, molecular inhibition (gene knockout or knockdown) is clearly more specific because pharmacological inhibitors of PCs still lack PC specificity (i.e., inhibit two or more PCs with equal potency). In regard to prostate cancer, various accepted human model cell lines have been previously well characterized. Therefore, for this study, we chose to establish the molecular inhibition of PACE4, using SOFA ribozyme technology, an exquisitely specific method of gene silencing, in the androgen-independent prostate cancer cell line DU145. After PACE4-SOFA-HDVRz transfection, a lower-than-expected number of stable cells were obtained, and transfected DU145 cells grew very slowly. In retrospect, based on all the evidence presented herein, this was most likely a direct consequence of lowered PACE4 levels, arguing a role of PACE4 in DU145 cell proliferation.

Considering the high selectivity of PACE4-SOFA-HDVRz, we chose the cell line with the lowest expression level of PACE4 mRNA for further studies (Figure 2*C*). Northern blots were performed for the other endogenously expressed PCs to illustrate that this effect was specific to PACE4 (Figure 2*D*). We also attempted to transfect the cell line with the lowest PACE4 levels with an expression vector containing the PACE4 cDNA. We were surprised to observe that PACE4 RNA levels were reestablished because this cell line still expressed the $tRNA^{Val}$-PACE4-SOFA-HDVRz (Figure 2*C*). This suggests that within a cellular context, the turnover rate of the ribozyme was not as high enough to affect a much larger pool of mRNA issued from expression vectors. Nonetheless, this partially reestablished cell line served our purpose as a control. We believed that this was the best control to use because it is directly derived from cells used for all experiments, eliminating all possible cell line–to–cell line variations. However, further improvements of the SOFA-HDVRz will eventually be required to reach higher turnover rates without significantly affecting its specificity.

To confirm that the established 4-2 cell line with lower PACE4 expression level was a suitable model of prostate cancer, we undertook a comparative gene expression profiling study (Figure 3). Among the downregulated genes in the 4-2 cell line, MUC1 is the one whose expression was the most affected by the PACE4 knockdown (Table W1). Mucin 1 is an oncoprotein expressed at high levels in diverse human carcinoma that is implicated in cellular transformation. Indeed, by its interactions with diverse effectors including EGFR, β-catenin, p53, IκN kinase, and NFκB p65, MUC1 blocks the induction of apoptosis and necrosis in human carcinoma [52,53]. A tissue microarray study reported the overexpressed of MUC1 in 58% of human primary prostate cancer tissues [58], whereas a correlation of its expression level in human prostate carcinoma tissues with the most advance stages of the disease was also reported [59]. The androgen-dependent prostate cancer cell line LNCaP does not express MUC1, the androgen-independent PC-3 cells expresses low constitutive levels, whereas DU145 cells highly and constitutively express MUC1 [52,60]. Our study now strongly correlates MUC1 expression with PACE4 expression level, as confirmed by quantitative PCR on the 4-2 cell line (Figure 3*B*) and immunohistochemical staining of DU145 and 4-2 tumor xenografts (Figure 5, *D* and *E*). Interestingly, the inhibition of MUC1 in DU145 cells with a peptide inhibitor interfering with its oligomerization led to similar effects than those reported in the present study for the 4-2 cell line; that is, inhibition of cell proliferation, induction of cell death pathways, and tumor regression of DU145 xenografts growing in nude mice [52].

Some of the effects reported in the present study could be directly linked to the reduced MUC1 expression caused by PACE4 inhibition, arguing for a central role of this overexpressed PCs in prostate carcinoma. Although this hypothesis needs further investigation, the study of MUC1 transcription regulators could lead to a better understanding of PACE4 contribution to its expression control, such as with known transcriptional regulators of MUC1 include TNF-α, IL-6, IFN-γ, TGF-β1, and HIF1-α [53]. In addition to TGF-β1, a known PC substrate [26], PACE4 could also regulate MUC1 expression indirectly by activating metalloproteinases such as ADAM17/TACE [61], which is directly involved into the regulation of TNF-α and IL-6 receptor [3]. Thus, considering the broad spectrum of potential endogenous substrates of PACE4, further investigations of its direct or indirect actions on the transcriptional control of these genes will be needed to better understand the gene expression profile of 4-2 cells.

The consequences of lowered levels of PACE4 are well illustrated by the reduced cell proliferation rate and the incapacity of these cells to form subcutaneous tumors in nude mice (Figures 4 and 5, respectively). The partial restoration of PACE4 expression levels in this cell line allowed a partial recovery of the *in vitro* proliferation rate, suggesting that PACE4 is a key player for tumoral growth and its expression levels have to be high to achieve this function (Figure 4). These results are in great agreement with the reduced levels of the CDK4 protein in the tumor derived from the 4-2 cell line compared with those found in the tumor derived from the DU145 cell line (Figure 5, *F* and *G*) because this protein is known to control the cell cycle. Moreover, analysis of the cell cycle in the DU145, 4-2 and 4-2 + PACE4 cell lines revealed the importance of PACE4 in regulating apoptosis and the cell cycle (Figure 6*A*). These results also indicated that partial recovery of PACE4 expression blocked DU145 apoptosis but could not reverse the blockade of cells into the G_0-G_1 phase, suggesting that full PACE4 activity is necessary to sustain the high proliferative state of DU145 cells.

In an attempt to identify other biomarkers affected by PACE4 in the proliferation of DU145 cells, we undertook proteomic analyses of DU145 and 4-2 cells derived conditioned media (Figure 6, *B* and *C*). In the samples issued from 4-2 cells, a fragment derived from the tryptic digestion of TRPS1 (a multitype zinc finger GATA-type transcription factor) was consistently detected [56]. This transcriptional repressor, whose expression is regulated by androgens through the androgen receptor, is normally expressed in the androgen-dependent LNCaP prostate cancer cells [62,63]. Its lack of expression has been previously reported for the androgen-independent DU145 prostate cancer cells [62], but the stable expression of recombinant TRPS1 in those cells allowed identification of both downregulated antiapoptotic protein POR2 and upregulated proapoptotic protein KAD2 [64]. Our data demonstrate that PACE4 can regulate the expression of the proapoptotic factor TRPS1. Further studies will be required to better characterize the involvement of PACE4 into the transcriptional control of the TRPS1 transcriptional repressor. As mentioned earlier, TRPS1 transcription is known to be regulated by androgens in cells LNCaP prostate cancer cells but not in the DU145 cell line, whose growth is independent of androgens and does not express the androgen receptor [62]. Recently, the bone morphogenic protein 7 (BMP-7), a growth factor belonging to the family of TGF-β that requires a PC cleavage for its propeptide removal [65], has been identified as an inducer of TRPS1 gene expression in mouse kidneys [66]. Thus, further characterization of the TRPS1 genetic regulation by BMP-7 in DU145, or other members of the TGF-β growth factor family that also need furin-like cleavages for processing [3], would be indicated to better understand the cellular functions of the overexpressed PACE4 in human prostate cancer cells.

The genes known to be transcriptionally regulated by TRPS1 include PSA [63], STAT3 [67], parathyroid hormone-related protein (PTHrP) [68], and osteocalcin [69]. Interestingly, the cleavage of human PTHrP and osteocalcin propeptides, essential for the generation of their mature forms, occurs at typical PCs processing sites ($_{31}$SRRLKR↓AV$_{38}$ and $_{46}$VKRPRR↓YL$_{51}$, respectively). Thus, the implication of PACE4 catalytic activity to the transcriptional control of TRPS1 and DU145 apoptosis triggering could be through these potential substrates. This hypothesis is supported by our genomic analysis, where the gene *PTHLH* (coding for PTHrP) was upregulated in 4-2 cells (Table W2).

Regarding the potential therapeutic avenues targeting PACE4, these include various approaches such as small molecule inhibitors [28], monoclonal antibodies [70], or even ribozymes or siRNA complexed with liposomes [71]. Small molecule inhibitors may be problematic because none of these have been shown to be specific to a particular PC. This is due to the high similarity of the catalytic regions of each PC. Whereas monoclonal antibodies could provide better specificity, it is not clear whether PACE4 localized at the cell surface and/or intracellular PACE4 will require targeting [72]. Finally, ribozyme or siRNA complexed with liposomes would certainly be highly specific but require additional research to make these reagents druggable. One potential avenue of research that offers both specificity and cell compatible characteristics (i.e., little toxicity and cell permeability) is the development of small peptide inhibitors (~1000 Da) targeting PACE4 [9]. Combined with peptidomimetics, such studies could lead to the development of novel drugs for prostate cancer.

In conclusion, this study reports the specific overexpression of PACE4 in prostate cancer tissues. Our results showed that PACE4 plays a major role in the progression of prostate tumors to a higher aggressive status, and its inhibition leads to a significant loss of tumorigenicity of the prostate tumor cell line DU145. A better understanding of PACE4 direct and indirect cellular targets contributing to these phenomena remains a great challenge and implicates multiple known oncogenic factors. Nonetheless, the data strongly validate PACE4 as an important therapeutic target in human prostate cancer.

Acknowledgments

The authors thank B. Cochan-Priollet (Hospital Lariboisiere, Paris, France) for the histopathological examination of prostate tissues. The authors also want to thank Xue-Wen Yuan for the technical assistance and Roxane Desjardins for the helpful discussions.

References

[1] Hanahan D and Weinberg RA (2000). The hallmarks of cancer. *Cell* **100**, 57–70.

[2] Bassi DE, Fu J, Lopez de Cicco R, and Klein-Szanto AJ (2005). Proprotein convertases: "master switches" in the regulation of tumor growth and progression. *Mol Carcinog* **44**, 151–161.

[3] Khatib AM, Siegfried G, Chretien M, Metrakos P, and Seidah NG (2002). Proprotein convertases in tumor progression and malignancy: novel targets in cancer therapy. *Am J Pathol* **160**, 1921–1935.

[4] Blanchard A, Iwasiow B, Yarmill A, Fresnosa A, Silha J, Myal Y, Murphy LC, Chretien M, Seidah N, and Shiu RP (2009). Targeted production of proprotein convertase PC1 enhances mammary development and tumorigenesis in transgenic mice. *Can J Physiol Pharmacol* **87**, 831–838.

[5] de Cicco RL, Bassi DE, Benavides F, Conti CJ, and Klein-Szanto AJ (2007). Inhibition of proprotein convertases: approaches to block squamous carcinoma development and progression. *Mol Carcinog* **46**, 654–659.

[6] Page RE, Klein-Szanto AJ, Litwin S, Nicolas E, Al-Jumaily R, Alexander P, Godwin AK, Ross EA, Schilder RJ, and Bassi DE (2007). Increased expression of the pro-protein convertase furin predicts decreased survival in ovarian cancer. *Cell Oncol* **29**, 289–299.

[7] Scamuffa N, Siegfried G, Bontemps Y, Ma L, Basak A, Cherel G, Calvo F, Seidah NG, and Khatib AM (2008). Selective inhibition of proprotein convertases represses the metastatic potential of human colorectal tumor cells. *J Clin Invest* **118**, 352–363.

[8] Bassi DE, Zhang J, Cenna J, Litwin S, Cukierman E, and Klein-Szanto AJ (2010). Proprotein convertase inhibition results in decreased skin cell proliferation, tumorigenesis, and metastasis. *Neoplasia* **12**, 516–526.

[9] Fugere M and Day R (2005). Cutting back on pro-protein convertases: the latest approaches to pharmacological inhibition. *Trends Pharmacol Sci* **26**, 294–301.

[10] Seidah NG, Mayer G, Zaid A, Rousselet E, Nassoury N, Poirier S, Essalmani R, and Prat A (2008). The activation and physiological functions of the proprotein convertases. *Int J Biochem Cell Biol* **40**, 1111–1125.

[11] Clark DA, Day R, Seidah N, Moody TW, Cuttitta F, and Davis TP (1993). Protease inhibitors suppress *in vitro* growth of human small cell lung cancer. *Peptides* **14**, 1021–1028.

[12] Mbikay M, Sirois F, Yao J, Seidah NG, and Chretien M (1997). Comparative analysis of expression of the proprotein convertases furin, PACE4, PC1 and PC2 in human lung tumours. *Br J Cancer* **75**, 1509–1514.

[13] Cheng M, Watson PH, Paterson JA, Seidah N, Chretien M, and Shiu RP (1997). Pro-protein convertase gene expression in human breast cancer. *Int J Cancer* **71**, 966–971.

[14] Tzimas GN, Chevet E, Jenna S, Nguyen DT, Khatib AM, Marcus V, Zhang Y, Chretien M, Seidah N, and Metrakos P (2005). Abnormal expression and processing of the proprotein convertases PC1 and PC2 in human colorectal liver metastases. *BMC Cancer* **5**, 149.

[15] Bassi DE, Mahloogi H, Al-Saleem L, Lopez De Cicco R, Ridge JA, and Klein-Szanto AJ (2001). Elevated furin expression in aggressive human head and neck tumors and tumor cell lines. *Mol Carcinog* **31**, 224–232.

[16] Fu Y, Campbell EJ, Shepherd TG, and Nachtigal MW (2003). Epigenetic regulation of proprotein convertase PACE4 gene expression in human ovarian cancer cells. *Mol Cancer Res* **1**, 569–576.

[17] Bassi DE, Lopez De Cicco R, Cenna J, Litwin S, Cukierman E, and Klein-Szanto AJ (2005). PACE4 expression in mouse basal keratinocytes results in basement membrane disruption and acceleration of tumor progression. *Cancer Res* **65**, 7310–7319.

[18] Bassi DE, Mahloogi H, Lopez De Cicco R, and Klein-Szanto A (2003). Increased furin activity enhances the malignant phenotype of human head and neck cancer cells. *Am J Pathol* **162**, 439–447.

[19] Hubbard FC, Goodrow TL, Liu SC, Brilliant MH, Basset P, Mains RE, and Klein-Szanto AJ (1997). Expression of PACE4 in chemically induced carcinomas is associated with spindle cell tumor conversion and increased invasive ability. *Cancer Res* **57**, 5226–5231.

[20] Mercapide J, Lopez De Cicco R, Bassi DE, Castresana JS, Thomas G, and Klein-Szanto AJ (2002). Inhibition of furin-mediated processing results in suppression of astrocytoma cell growth and invasiveness. *Clin Cancer Res* **8**, 1740–1746.

[21] Remacle AG, Rozanov DV, Fugere M, Day R, and Strongin AY (2006). Furin regulates the intracellular activation and the uptake rate of cell surface–associated MT1-MMP. *Oncogene* **25**, 5648–5655.

[22] Coppola JM, Bhojani MS, Ross BD, and Rehemtulla A (2008). A small-molecule furin inhibitor inhibits cancer cell motility and invasiveness. *Neoplasia* **10**, 363–370.

[23] McColl BK, Paavonen K, Karnezis T, Harris NC, Davydova N, Rothacker J, Nice EC, Harder KW, Roufail S, Hibbs ML, et al. (2007). Proprotein convertases promote processing of VEGF-D, a critical step for binding the angiogenic receptor VEGFR-2. *FASEB J* **21**, 1088–1098.

[24] Basak A, Khatib AM, Mohottalage D, Basak S, Kolajova M, and Bag SS (2009). A novel enediynyl peptide inhibitor of furin that blocks processing of proPDGF-A, B and proVEGF-C. *PLoS One* **4**, e7700.

[25] Siegfried G, Basak A, Prichett-Pejic W, Scamuffa N, Ma L, Benjannet S, Veinot JP, Calvo F, Seidah N, and Khatib AM (2005). Regulation of the stepwise proteolytic cleavage and secretion of PDGF-B by the proprotein convertases. *Oncogene* **24**, 6925–6935.

[26] Dubois CM, Blanchette F, Laprise MH, Leduc R, Grondin F, and Seidah NG (2001). Evidence that furin is an authentic transforming growth factor-β_1–converting enzyme. *Am J Pathol* **158**, 305–316.

[27] Basak A (2005). Inhibitors of proprotein convertases. *J Mol Med* **83**, 844–855.

[28] Komiyama T, Coppola JM, Larsen MJ, van Dort ME, Ross BD, Day R, Rehemtulla A, and Fuller RS (2009). Inhibition of furin/proprotein convertase-catalyzed surface and intracellular processing by small molecules. *J Biol Chem* **284**, 15729–15738.

[29] Becker GL, Sielaff F, Than ME, Lindberg I, Routhier S, Day R, Lu Y, Garten W, and Steinmetzer T (2010). Potent inhibitors of furin and furin-like proprotein convertases containing decarboxylated P1 arginine mimetics. *J Med Chem* **53**, 1067–1075.

[30] Coppola JM, Hamilton CA, Bhojani MS, Larsen MJ, Ross BD, and Rehemtulla A (2007). Identification of inhibitors using a cell-based assay for monitoring Golgi-resident protease activity. *Anal Biochem* **364**, 19–29.

[31] Uchida K, Chaudhary LR, Sugimura Y, Adkisson HD, and Hruska KA (2003). Proprotein convertases regulate activity of prostate epithelial cell differentiation markers and are modulated in human prostate cancer cells. *J Cell Biochem* **88**, 394–399.

[32] Tafech A, Bassett T, Sparanese D, and Lee CH (2006). Destroying RNA as a therapeutic approach. *Curr Med Chem* **13**, 863–881.

[33] Jemal A, Siegel R, Xu J, and Ward E (2010). Cancer statistics, 2010. *CA Cancer J Clin* **60**, 277–300.

[34] Fizazi K, Sternberg CN, Fitzpatrick JM, Watson RW, and Tabesh M (2010). Role of targeted therapy in the treatment of advanced prostate cancer. *BJU Int* **105**, 748–767.

[35] Chene L, Giroud C, Desgrandchamps F, Boccon-Gibod L, Cussenot O, Berthon P, and Latil A (2004). Extensive analysis of the 7q31 region in human prostate tumors supports TES as the best candidate tumor suppressor gene. *Int J Cancer* **111**, 798–804.

[36] Mellinger GT, Gleason D, and Bailar J III (1967). The histology and prognosis of prostatic cancer. *J Urol* **97**, 331–337.

[37] Schroder FH, Hermanek P, Denis L, Fair WR, Gospodarowicz MK, and Pavone-Macaluso M (1992). The TNM classification of prostate cancer. *Prostate Suppl* **4**, 129–138.

[38] Dong W, Seidel B, Marcinkiewicz M, Chretien M, Seidah NG, and Day R (1997). Cellular localization of the prohormone convertases in the hypothalamic paraventricular and supraoptic nuclei: selective regulation of PC1 in corticotrophin-releasing hormone parvocellular neurons mediated by glucocorticoids. *J Neurosci* **17**, 563–575.

[39] Lucier JF, Bergeron LJ, Briere FP, Ouellette R, Elela SA, and Perreault JP (2006). RiboSubstrates: a Web application addressing the cleavage specificities of ribozymes in designated genomes. *BMC Bioinformatics* **7**, 480.

[40] D'Anjou F, Bergeron LJ, Larbi NB, Fournier I, Salzet M, Perreault JP, and Day R (2004). Silencing of SPC2 expression using an engineered delta ribozyme in the mouse βTC-3 endocrine cell line. *J Biol Chem* **279**, 14232–14239.

[41] Creemers JW, Groot Kormelink PJ, Roebroek AJ, Nakayama K, and Van de Ven WJ (1993). Proprotein processing activity and cleavage site selectivity of the Kex2-like endoprotease PACE4. *FEBS Lett* **336**, 65–69.

[42] Denault JB, Lazure C, Day R, and Leduc R (2000). Comparative characterization of two forms of recombinant human SPC1 secreted from Schneider 2 cells. *Protein Expr Purif* **19**, 113–124.

[43] Seidah NG, Hamelin J, Mamarbachi M, Dong W, Tardos H, Mbikay M, Chretien M, and Day R (1996). cDNA structure, tissue distribution, and chromosomal localization of rat PC7, a novel mammalian proprotein convertase closest to yeast kexin-like proteinases. *Proc Natl Acad Sci USA* **93**, 3388–3393.

[44] Day R, Schafer MK, Watson SJ, Chretien M, and Seidah NG (1992). Distribution and regulation of the prohormone convertases PC1 and PC2 in the rat pituitary. *Mol Endocrinol* **6**, 485–497.

[45] Tusher VG, Tibshirani R, and Chu G (2001). Significance analysis of microarrays applied to the ionizing radiation response. *Proc Natl Acad Sci USA* **98**, 5116–5121.

[46] Tsuji A, Kanie H, Makise H, Yuasa K, Nagahama M, and Matsuda Y (2007). Engineering of α_1-antitrypsin variants selective for subtilisin-like proprotein convertases PACE4 and PC6: importance of the P2′ residue in stable complex formation of the serpin with proprotein convertase. *Protein Eng Des Sel* **20**, 163–170.

[47] Bergeron LJ and Perreault JP (2005). Target-dependent on/off switch increases ribozyme fidelity. *Nucleic Acids Res* **33**, 1240–1248.

[48] Bergeron LJ, Reymond C, and Perreault JP (2005). Functional characterization of the SOFA delta ribozyme. *RNA* **11**, 1858–1868.

[49] Levesque MV, Levesque D, Briere FP, and Perreault JP (2010). Investigating a new generation of ribozymes in order to target HCV. *PLoS One* **5**, e9627.

[50] Posthaus H, Dubois CM, and Muller E (2003). Novel insights into cadherin processing by subtilisin-like convertases. *FEBS Lett* **536**, 203–208.

[51] Nakajima T, Konda Y, Kanai M, Izumi Y, Kanda N, Nanakin A, Kitazawa S, and Chiba T (2002). Prohormone convertase furin has a role in gastric cancer cell proliferation with parathyroid hormone–related peptide in a reciprocal manner. *Dig Dis Sci* **47**, 2729–2737.

[52] Joshi MD, Ahmad R, Yin L, Raina D, Rajabi H, Bubley G, Kharbanda S, and Kufe D (2009). MUC1 oncoprotein is a druggable target in human prostate cancer cells. *Mol Cancer Ther* **8**, 3056–3065.

[53] Jonckheere N and Van Seuningen I (2010). The membrane-bound mucins: From cell signalling to transcriptional regulation and expression in epithelial cancers. *Biochimie* **92**, 1–11.

[54] Zhu H, Mao Q, Lin Y, Yang K, and Xie L (2010). RNA interference targeting mutant p53 inhibits growth and induces apoptosis in DU145 human prostate cancer cells. *Med Oncol*, E-pub: September 21, 2010.

[55] Wang Q, Zheng JY, Kreth J, Yan X, Kamata M, Campbell RA, Xie Y, Chiu R, Berenson JR, Shi W, et al. (2009). Regulation of prostate-specific antigen expression by the junctional adhesion molecule A. *Urology* **73**, 1119–1125.

[56] Chang GT, van den Bemd GJ, Jhamai M, and Brinkmann AO (2002). Structure and function of GC79/TRPS1, a novel androgen-repressible apoptosis gene. *Apoptosis* **7**, 13–21.

[57] Malik TH, Shoichet SA, Latham P, Kroll TG, Peters LL, and Shivdasani RA (2001). Transcriptional repression and developmental functions of the atypical vertebrate GATA protein TRPS1. *EMBO J* **20**, 1715–1725.

[58] Cozzi PJ, Wang J, Delprado W, Perkins AC, Allen BJ, Russell PJ, and Li Y (2005). MUC1, MUC2, MUC4, MUC5AC and MUC6 expression in the progression of prostate cancer. *Clin Exp Metastasis* **22**, 565–573.

[59] Kirschenbaum A, Itzkowitz SH, Wang JP, Yao S, Eliashvili M, and Levine AC (1999). MUC1 expression in prostate carcinoma: correlation with grade and stage. *Mol Urol* **3**, 163–168.

[60] O'Connor JC, Julian J, Lim SD, and Carson DD (2005). MUC1 expression in human prostate cancer cell lines and primary tumors. *Prostate Cancer Prostatic Dis* **8**, 36–44.

[61] Srour N, Lebel A, McMahon S, Fournier I, Fugere M, Day R, and Dubois CM (2003). TACE/ADAM-17 maturation and activation of sheddase activity require proprotein convertase activity. *FEBS Lett* **554**, 275–283.

[62] Chang GT, Jhamai M, van Weerden WM, Jenster G, and Brinkmann AO (2004). The TRPS1 transcription factor: androgenic regulation in prostate cancer and high expression in breast cancer. *Endocr Relat Cancer* **11**, 815–822.

[63] van den Bemd GJ, Jhamai M, Brinkmann AO, and Chang GT (2003). The atypical GATA protein TRPS1 represses androgen-induced prostate-specific antigen expression in LNCaP prostate cancer cells. *Biochem Biophys Res Commun* **312**, 578–584.

[64] Chang GT, Gamble SC, Jhamai M, Wait R, Bevan CL, and Brinkmann AO (2007). Proteomic analysis of proteins regulated by TRPS1 transcription factor in DU145 prostate cancer cells. *Biochim Biophys Acta* **1774**, 575–582.

[65] Swencki-Underwood B, Mills JK, Vennarini J, Boakye K, Luo J, Pomerantz S, Cunningham MR, Farrell FX, Naso MF, and Amegadzie B (2008). Expression and characterization of a human BMP-7 variant with improved biochemical properties. *Protein Expr Purif* **57**, 312–319.

[66] Gai Z, Zhou G, Itoh S, Morimoto Y, Tanishima H, Hatamura I, Uetani K, Ito M, and Muragaki Y (2009). Trps1 functions downstream of Bmp7 in kidney development. *J Am Soc Nephrol* **20**, 2403–2411.

[67] Suemoto H, Muragaki Y, Nishioka K, Sato M, Ooshima A, Itoh S, Hatamura I, Ozaki M, Braun A, Gustafsson E, et al. (2007). Trps1 regulates proliferation and apoptosis of chondrocytes through Stat3 signaling. *Dev Biol* **312**, 572–581.

[68] Nishioka K, Itoh S, Suemoto H, Kanno S, Gai Z, Kawakatsu M, Tanishima H, Morimoto Y, Hatamura I, Yoshida M, et al. (2008). Trps1 deficiency enlarges the proliferative zone of growth plate cartilage by upregulation of Pthrp. *Bone* **43**, 64–71.

[69] Piscopo DM, Johansen EB, and Derynck R (2009). Identification of the GATA factor TRPS1 as a repressor of the osteocalcin promoter. *J Biol Chem* **284**, 31690–31703.

[70] Chan JC, Piper DE, Cao Q, Liu D, King C, Wang W, Tang J, Liu Q, Higbee J, Xia Z, et al. (2009). A proprotein convertase subtilisin/kexin type 9 neutralizing antibody reduces serum cholesterol in mice and nonhuman primates. *Proc Natl Acad Sci USA* **106**, 9820–9825.

[71] Shim MS and Kwon YJ (2010). Efficient and targeted delivery of siRNA *in vivo*. *FEBS J* **277**, 4814–4827.

[72] Mayer G, Hamelin J, Asselin MC, Pasquato A, Marcinkiewicz E, Tang M, Tabibzadeh S, and Seidah NG (2008). The regulated cell surface zymogen activation of the proprotein convertase PC5A directs the processing of its secretory substrates. *J Biol Chem* **283**, 2373–2384.

Table W1. Downregulated Genes in 4-2 Cells Compared to DU145.

Accession Numbers	Gene Symbol	Gene Description	Fold Change DU145 *vs* 4-2	*P*
NM_002456	*MUC1*	Mucin 1	0.080	.00123
NM_030631	*SLC25A21*	Solute carrier family 25 (mitochondrial oxodicarboxylate carrier), member 21	0.118	.00037
NM_021034	*IFITM3*	Interferon-induced transmembrane protein 3 (1-8U)	0.121	.00038
NM_006435	*IFITM2*	Interferon-induced transmembrane protein 2 (1-8D)	0.142	.00109
NM_004613	*TGM2*	Transglutaminase 2	0.182	.00043
NM_013230	*CD24*	CD24	0.184	.02952
NM_019601	*SUSD2*	Sushi domain containing 2	0.186	.01475
NM_004657	*SDPR*	serum deprivation response	0.209	.01243
XM_938803	*CST6*	Cystatin E/M	0.282	.02171
NM_052886	*MAL2*	mal, T-cell differentiation protein 2	0.302	.00003
NM_001430	*EPAS1*	Endothelial PAS domain protein 1	0.313	.00121
NM_000101	*CYBA*	Cytochrome *b*-245, α polypeptide	0.314	.02607
NM_001038	*SCNN1A*	Sodium channel, non–voltage-gated 1α	0.317	.00156
NM_032899	*FAM83A*	Family with sequence similarity 83, member A	0.319	.00745
NM_000211	*ITGB2*	Integrin, β_2	0.324	.00416
NM_001386	*DPYSL2*	Dihydropyrimidinase-like 2	0.325	.00857
NM_003280	*TNNC1*	Troponin C type 1 (slow)	0.328	.03211
NM_001823	*CKB*	Creatine kinase, brain	0.347	.01088
NM_174911	*FAM84B*	Family with sequence similarity 84, member B	0.353	.00069
NM_001793	*CDH3*	Cadherin 3	0.354	.00003
NM_007257	*PNMA2*	Paraneoplastic antigen MA2	0.358	.00459
NM_021135	*RPS6KA2*	Ribosomal protein S6 kinase	0.367	.00103
NM_020859	*SHRM*	Shroom	0.369	.00973
NM_199001	*MGC59937*	Similar to RIKEN cDNA 2310002J15 gene	0.374	.00505
NM_001003794	*MGLL*	Monoglyceride lipase	0.375	.00604
NM_003246	*THBS1*	Thrombospondin 1	0.394	.03839
NM_004360	*CDH1*	Cadherin 1	0.399	.00005
NM_002754	*MAPK13*	Mitogen-activated protein kinase 13	0.400	.00182
NM_002354	*TACSTD1*	Tumor-associated calcium signal transducer 1	0.402	.00197
NM_173584	*MGC45840*	EF-hand calcium binding domain 4A	0.406	.00659
AK027147	*HS.509165*	cDNA: FLJ23494 fis, clone LNG01885	0.407	.00691
NM_014578	*RHOD*	ras homolog gene family, member D	0.409	.00604
NM_182498	*C19ORF37*	Zinc finger protein 428	0.416	.00178
XM_051862	*LOC58489*	Hypothetical protein from EUROIMAGE 588495	0.416	.02740
NM_020210	*SEMA4B*	Semaphorin 4B	0.417	.02468
NM_020770	*CGN*	Cingulin	0.419	.04416
NM_024329	*EFHD2*	EF-hand domain family, member D2	0.430	.00365
NM_019058	*DDIT4*	DNA-damage-inducible transcript 4	0.431	.03417
NM_024830	*AYTL2*	Acyltransferase like 2	0.437	.00391
NM_198282	*TMEM173*	Transmembrane protein 173	0.437	.00316
NM_005630	*SLCO2A1*	Solute carrier organic anion transporter family, member 2A1	0.437	.00219
NM_015055	*SWAP70*	SWAP-70 protein	0.442	.00778
NM_021101	*CLDN1*	Claudin 1	0.443	.01301
NM_017917	*PPP2R3C*	Protein phosphatase 2, regulatory subunit B″, γ	0.444	.00839
NM_005195	*CEBPD*	CCAAT/enhancer binding protein	0.457	.03235
NM_018478	*C20ORF35*	Chromosome 20 open reading frame 35	0.461	.01029
NM_021818	*SAV1*	Salvador homolog 1	0.467	.00302
NM_000600	*IL6*	Interleukin 6	0.467	.04991
NM_014220	*TM4SF1*	Transmembrane 4 L six family member 1	0.479	.00002
BU536065	*HS.579631*	cDNA clone IMAGE: 6563923 5, mRNA sequence	0.485	.03222
NM_003475	*RASSF7*	Ras association (RalGDS/AF-6) domain family 7	0.488	.00515
NM_001013398	*IGFBP3*	Insulin-like growth factor binding protein 3	0.490	.02959
NM_025151	*RAB11FIP1*	RAB11 family interacting protein 1 (class I)	0.490	.04771
NM_033317	*ZD52F10*	Dermokine	0.493	.00677
NM_001993	*F3*	Coagulation factor III	0.494	.00051
NM_006169	*NNMT*	Nicotinamide *N*-methyltransferase	0.495	.00990
NM_003726	*SCAP1*	src family associated phosphoprotein 1	0.496	.00242
XM_944693	*ITGB5*	Integrin, β_5	0.496	.00388
NM_018098	*ECT2*	Epithelial cell- transforming sequence 2 oncogene	0.498	.00104

Table W2. Upregulated Genes in 4-2 Cells Compared to DU145.

Accession Numbers	Gene Symbol	Gene Description	Fold Change DU145 *vs* 4-2	*P*
NM_006216	*SERPINE2*	Serpin peptidase inhibitor, clade E, member 2	5.140	.02748
NM_005242	*F2RL1*	Coagulation factor II (thrombin) receptor-like 1	5.119	.00063
NM_014689	*DOCK10*	Dedicator of cytokinesis 10	4.418	.00296
NM_178012	*TUBB2B*	Tubulin, β_{2B}	4.330	.00075
NM_024101	*MLPH*	Melanophilin	4.310	.00118
NM_003937	*KYNU*	Kynureninase	3.722	.03011
NM_002281	*KRTHB1*	Keratin 81	3.623	.01352
NM_003739	*AKR1C3*	Aldo-keto reductase family 1, member C3	3.488	.00293
NM_177949	*ARMCX2*	Armadillo repeat containing, X-linked 2	3.079	.00010
NM_002522	*NPTX1*	Neuronal pentraxin I	2.988	.00034
NM_024016	*HOXB8*	Homeo box B8	2.911	.00218
NM_000104	*CYP1B1*	Cytochrome P450, family 1, subfamily B, polypeptide 1	2.866	.00415
NM_002380	*MATN2*	Matrilin 2	2.854	.00584
NM_000165	*GJA1*	Gap junction protein, α_1	2.833	.00032
NM_020299	*AKR1B10*	Aldo-keto reductase family 1, member B10	2.830	.00556
NM_153344	*C6ORF141*	Chromosome 6 open reading frame 141	2.727	.01479
NM_002228	*JUN*	jun oncogene	2.655	.00128
NM_004163	*RAB27B*	Clone 25194 mRNA sequence	2.615	.01647
NM_004398	*DDX10*	DEAD (Asp-Glu-Ala-Asp) box polypeptide 10	2.593	.00221
NM_000782	*CYP24A1*	Cytochrome P450, family 24, subfamily A, polypeptide 1	2.504	.00226
NM_001259	*CDK6*	Cyclin-dependent kinase 6	2.461	.00582
NM_020919	*ALS2*	Amyotrophic lateral sclerosis 2 (juvenile)	2.439	.00248
NM_001964	*EGR1*	Early growth response 1	2.438	.01511
AF131834	*HS.4892*	Clone 24841	2.428	.00563
NM_003543	*HIST1H4H*	Histone cluster 1, H4h	2.413	.01138
NM_002639	*SERPINB5*	Serpin peptidase inhibitor, clade B, member 5	2.406	.00149
NM_012419	*RGS17*	Regulator of G-protein signaling 17	2.351	.01676
NM_032784	*RSPO3*	R-spondin 3 homolog	2.348	.03649
XM_928153	*LOC653571*	Similar to sperm protein associated with the nucleus, X chromosome, family member B1	2.329	.00901
NM_002737	*PRKCA*	Protein kinase C, α	2.326	.00476
NM_001001390	*CD44*	CD44 molecule (Indian blood group)	2.306	.01926
XM_940680	*LOC648517*	Similar to aldo-keto reductase family 1 member C1	2.269	.01923
NM_003528	*HIST2H2BE*	Histone cluster 2, H2be	2.264	.00707
NM_003714	*STC2*	Stanniocalcin 2	2.261	.02278
NM_012242	*DKK1*	Dickkopf homolog 1	2.249	.00873
NM_020547	*AMHR2*	Anti-mullerian hormone receptor, type II	2.213	.00011
AK091904	*HS.202577*	cDNA FLJ34585 fis, clone KIDNE2008758	2.202	.00825
NM_198966	*PTHLH*	Parathyroid hormone-like hormone	2.200	.00008
NM_015508	*TIPARP*	TCDD-inducible poly(ADP-ribose) polymerase	2.190	.02173
NM_001236	*CBR3*	Carbonyl reductase 3	2.175	.00163
NM_001387	*DPYSL3*	Dihydropyrimidinase-like 3	2.165	.01420
NM_025145	*C10ORF79*	Chromosome 10 open reading frame 79	2.158	.00026
NM_001889	*CRYZ*	Crystallin, zeta (quinone reductase)	2.151	.01170
NM_004403	*DFNA5*	Deafness, autosomal dominant 5	2.141	.00460
NM_005319	*HIST1H1C*	Histone cluster 1, H1c	2.110	.00689
NM_001878	*CRABP2*	Cellular retinoic acid binding protein 2	2.094	.01508
NM_001010924	*C10ORF38*	Chromosome 10 open reading frame 38	2.092	.00581
NM_000475	*NR0B1*	Nuclear receptor subfamily 0, group B, member 1	2.084	.00179
NM_004615	*TSPAN7*	Tetraspanin 7	2.084	.00504
NM_000358	*TGFBI*	Transforming growth factor, β-induced	2.057	.02546
NM_005329	*HAS3*	Hyaluronan synthase 3	2.051	.03194
NM_032168	*WDR75*	WD repeat domain 75	2.020	.01148
NM_001008490	*KLF6*	Kruppel-like factor 6	2.018	.00732
NM_006120	*HLA-DMA*	Major histocompatibility complex, class II, DM α	2.018	.02250
XM_937100	*KRTAP2-1*	Keratin-associated protein 2-1	2.013	.01978
NM_002178	*IGFBP6*	Insulin-like growth factor binding protein 6	2.009	.01644
NM_005682	*GPR56*	G protein–coupled receptor 56	2.009	.01484
NM_006307	*SRPX*	Sushi-repeat–containing protein, X-linked	2.009	.00006
NM_002147	*HOXB5*	Homeo box B5	2.006	.00202
NM_015642	*ZBTB20*	Zinc finger and BTB domain containing 20	2.005	.01040
NM_020411	*XAGE1*	X antigen family, member 1D	2.002	.02842
NM_016352	*CPA4*	Carboxypeptidase A4	2.000	.03194